haematologica
Journal of The Ferrata Storti Foundation

Burkitt-like lymphoma with 11q aberration: a germinal center derived lymphoma genetically unrelated to Burkitt lymphoma

by Blanca Gonzalez-Farre, Joan Enric Ramis-Zaldivar, Julia Salmeron-Villalobos, Olga Balagué, Verónica Celis, Jaime Verdu-Amoros, Ferran Nadeu, Constantino Sábado, Antonio Ferrández, Marta Garrido, Federico García-Bragado, María Dolores de la Maya, José Manuel Vagace, Carlos Manuel Panizo, Itziar Astigarraga, Mara Andrés, Elaine S. Jaffe, Elias Campo, and Itziar Salaverria

Haematologica 2019 [Epub ahead of print]

Citation: Blanca Gonzalez-Farre, Joan Enric Ramis-Zaldivar, Julia Salmeron-Villalobos, Olga Balagué, Verónica Celis, Jaime Verdu-Amoros, Ferran Nadeu, Constantino Sábado, Antonio Ferrández, Marta Garrido, Federico García-Bragado, María Dolores de la Maya, José Manuel Vagace, Carlos Manuel Panizo, Itziar Astigarraga, Mara Andrés, Elaine S. Jaffe, Elias Campo, and Itziar Salaverria. Burkitt-like lymphoma with 11q aberration: a germinal center derived lymphoma genetically unrelated to Burkitt lymphoma.
Haematologica. 2019; 104:xxx
doi:10.3324/haematol.2018.207928

Burkitt-like lymphoma with 11q aberration: A germinal center derived lymphoma genetically unrelated to Burkitt lymphoma

Blanca Gonzalez-Farre,[1,2,3*] Joan Enric Ramis-Zaldivar,[2,3*] Julia Salmeron-Villalobos,[2] Olga Balagué,[1,2,3] Verónica Celis,[4] Jaime Verdu-Amoros,[5] Ferran Nadeu,[2,3] Constantino Sábado,[6] Antonio Ferrández,[7] Marta Garrido,[8] Federico García-Bragado,[9] María Dolores de la Maya,[10] José Manuel Vagace,[10] Carlos Manuel Panizo,[11] Itziar Astigarraga,[12] Mara Andrés,[13] Elaine S Jaffe,[14] Elias Campo,[1,2,3+] and Itziar Salaverria [2,3+]

[1] Hematopathology Unit, Hospital Clínic de Barcelona, University of Barcelona, Barcelona, Spain
[2] Institut d'Investigacions Biomèdiques August Pi i Sunyer (IDIBAPS), Barcelona, Spain
[3] Centro de Investigación Biomédica en Red de Cáncer (CIBERONC), Spain
[4] Pediatric Oncology Department, Hospital Sant Joan de Déu, Esplugues de Llobregat, Spain
[5] Pediatric Oncology Department, Hospital Clínico Universitario de Valencia, Valencia, Spain
[6] Pediatric Oncology Department, Hospital Universitari Vall d'Hebron, Barcelona, Spain
[7] Pathology Department, Hospital Clínico de Valencia, Valencia, Spain
[8] Pathology Department, Hospital Universitari Vall d'Hebron, Barcelona, Spain
[9] Pathology Department, Complejo Hospitalario de Navarra, Pamplona, Spain
[10] Pediatric Hematology Department, Hospital Materno Infantil de Badajoz, Badajoz, Spain
[11] Department of Hematology, Clínica Universidad de Navarra and Instituto de Investigación Sanitaria de Navarra (IdiSNA), Pamplona, Spain
[12] Pediatrics Department, Hospital Universitario Cruces, IIS Biocruces Bizkaia, UPV/EHU, Barakaldo, Spain
[13] Pediatric Oncology Department, Hospital La Fe, Valencia, Spain
[14] Hematopathology Section, Laboratory of Pathology, National Cancer Institute, National Institutes of Health, Bethesda, MD

*BGF, JERZ and [+]EC, IS contributed equally to this study.

Running Title: Burkitt-like lymphoma with 11q aberration

Corresponding Author: Itziar Salaverria, Institut d'Investigacions Biomèdiques August Pi i Sunyer (IDIBAPS), Rosselló 149-153, 08036-Barcelona, Spain, Phone +34932275400, Ext 4582, Fax +34932275572; email: isalaver@clinic.cat

Word Count: Abstract: 218, Main Text: 3384

Figures: 2, Table: 1, References: 31, Supplemental files: 3

Funding

This work was supported by Asociación Española Contra el Cáncer (AECC CICPFI6025SALA), Fondo de Investigaciones Sanitarias Instituto de Salud Carlos III (Miguel Servet program CP13/00159 and PI15/00580, I.S.), Spanish Ministerio de Economía y Competitividad, Grant SAF2015-64885-R(EC), Generalitat de Catalunya Suport Grups de Recerca (2017-SGR-1107 I.S. and 2017-SGR-1142 E.C.), and the European Regional Development Fund “Una manera de fer Europa”. J.E.R-Z was supported by a fellowship from Generalitat de Catalunya AGAUR FI-DGR 2017 (2017 FI_B01004). E.C. is an Academia Researcher of the "Institució Catalana de Recerca i Estudis Avançats" (ICREA) of the Generalitat de Catalunya. This work was developed at the Centro Esther Koplowitz, Barcelona, Spain. The group is supported by Acció instrumental d’incorporació de científics i tecnòlegs PERIS 2016 (SLT002/16/00336) from Generalitat de Catalunya.

The copy-number data reported in this article have been deposited at GEO database under accession number GSE116527. Sequencing data have been deposited at the European Nucleotide Archive (ENA, accession number ERP110085).

Acknowledgments

We thank the centers of the Sociedad Española de Hematología y Oncología Pediátricas that submitted cases for consultation and Noelia Garcia, Silvia Martín, and Helena Suarez for their excellent technical assistance. We are indebted to the IDIBAPS Genomics Core Facility and to HCB-IDIBAPS Biobank-Tumor Bank and Biobanc de l’Hospital Infantil Sant Joan de Déu, both integrated in the National Network Biobanks of ISCIII for the sample and data procurement. We thank Prof. Reiner Siebert from the University of Ulm to share 11q FISH probe design.

ABSTRACT

Burkitt-like lymphoma with 11q aberration is characterized by pathological features and gene expression profile resembling Burkitt lymphoma but lack *MYC* rearrangement and carries an 11q-arm aberration with proximal gains and telomeric losses. Whether these lymphomas are a distinct category or a particular variant of other recognized entities is controversial. To improve the understanding of Burkitt-like lymphoma with 11q aberration we have performed an analysis of copy number alterations and targeted sequencing of a large panel of B-cell lymphoma related genes in 11 cases. Most patients had localized nodal disease and a favorable outcome after therapy. Histologically, they were high grade B-cell lymphoma, not otherwise specified (8 cases), diffuse large B-cell lymphoma (2 cases) and only one was considered as atypical Burkitt lymphoma. All cases had a germinal center B-cell signature and phenotype with frequent LMO2 expression. Burkitt-like lymphoma with 11q aberration had frequent gains of 12q12-q21.1 and losses of 6q12.1-q21, and lacked common Burkitt lymphoma or diffuse large B-cell lymphoma alterations. Potential driver mutations were found in 27 genes, particularly involving *BTG2, DDX3X, ETS1, EP300,* and *GNA13.* However, *ID3*, *TCF3*, or *CCND3* mutations were absent in all cases. These results suggest that Burkitt-like lymphoma with 11q aberration is a germinal center derived lymphoma closer to high grade B-cell lymphoma or diffuse large B-cell lymphoma rather than Burkitt lymphoma.

Introduction

Our knowledge of pediatric and young adults lymphomas has dramatically increased in the last years with the identification of several subtypes that predominantly occur in this subgroup of age.[1-4] One of these recently recognized categories is Burkitt-like lymphoma with 11q aberration (BLL-11q) which morphological, phenotypic, and gene expression profile resemble Burkitt lymphoma (BL), but they lack *MYC* rearrangements by standard detection methods as fluorescence *in situ* hybridization (FISH). Alternatively, these tumors carry an 11q-arm aberration characterized by proximal gains and telomeric losses.[4] In comparison with BL, these lymphomas seem to have more complex karyotypes, a certain degree of cytological pleomorphism, sporadically a follicular pattern and high incidence of nodal presentation.[4,5] Very similar cases have also been reported in the post-transplant setting,[6] although its incidence in other immunocompromised conditions as HIV is still unclear.[7,8]

BLL-11q has been incorporated in the revised WHO classification as a provisional category[1] because its precise taxonomy as a particular variant of BL, diffuse large B-cell lymphoma (DLBCL) or a distinct form of high grade B-cell lymphoma (HGBCL) is still controversial.[1,4-6,9-11] The clarification of the biological nature of this uncommon lymphoma subtype is clinically relevant due to increasing interest in defining the most appropriate management strategies for specific subtypes of lymphomas in pediatric and young adults patients.[12] Recent DNA copy number alteration (CNA) and next-generation sequencing (NGS) studies have provided a comprehensive catalog of genomic aberrations in BL and DLBCL that clearly distinguish these entities.[13-17] In this study we have performed an integrated analysis of genomic and mutational alterations with a complete annotation of clinical and pathological features of BLL-11q with the goal of obtaining insights to refine the understanding of the pathogenesis and improve the diagnosis of these tumors.

Methods

Sample selection and DNA/RNA extraction

To identify BLL-11q cases we initially reevaluated the presence of *MYC* translocation in 95 cases diagnosed as BL, atypical BL or HGBCL, not otherwise specified (NOS), in our Hematopathology Unit between 2000-2016. Three consultation cases from centers belonging to Sociedad Española de Hematología y Oncología Pediátricas (SEHOP) were also analyzed. Cases were reviewed by three pathologists (BG-F, EC, ESJ). DNA and RNA were extracted using standard protocols (Qiagen, Hilden, Germany). This study was approved by the Institutional Review Board of the Hospital Clinic of Barcelona. Informed consent was obtained from all patients in accordance with the Declaration of Helsinki.

Immunohistochemistry and FISH

Immunohistochemical analysis using a panel of antibodies detecting common B and T cell markers as well as LMO2 and MYC was performed and interpreted as previously reported (**Online Supplementary Table S1**).[18,19]

MYC breaks and *MYC*/IGH fusions were analyzed by FISH using XL MYC BA Probe (Metasystems, Altlussheim, Germany) and LSI IGH/MYC/CEP 8 Tri-Color Dual Fusion Probe Kit (Vysis-Abbott, Abbott Park, IL) respectively. The 11q alteration was studied with a custom FISH probe using BAC clones (Invitrogen inc.) for proximal gains (RP11-414G21-spectrum green) and terminal losses (RP11-629A20-spectrum red) combined with CEP11-spectrum aqua (Vysis-Abbott inc.). The FISH constellation in a normal case is characterized by two signals per probe, while the pattern corresponding to the 11q gain/loss or gain/amplification/loss aberration would be two blue, three up to five green signals and one red signal. The probe was tested in an independent series of 8 non-Hodgkin B-cell lymphomas and 4 *MYC*-negative HGBCL with lack of the 11q alteration by array and all showed the normal pattern described above.

Copy number analysis

DNAs were hybridized on Oncoscan FFPE or SNP array platform (ThermoFisher Scientific, Waltham, MA) and analyzed as described previously (**Online Supplementary Methods**).[2] Published CN data on *MYC*-positive BL[20] and DLBCL[13] were reanalyzed for comparison.

Sequencing approaches

The mutational status of 96 B-cell lymphoma related genes (**Online Supplementary Table S2**) was examined by target NGS in 10 BLL-11q cases and 4 *MYC*-negative 11q-negative cases using a NGS SureSelect XT Target Enrichment System Capture strategy (Agilent Technologies, Santa Clara, CA) before sequencing in a MiSeq instrument (Illumina, San Diego, CA) **(Online Supplementary Methods)**. Additionally, analysis of hotspots of mutation in *ID3*, *TCF3* and *CCND3* genes, *ETS1* exon 1 (transcript NM_005238) and verification of variants in specific cases was performed by Sanger sequencing using primers described in **Online Supplementary Table S3.**

Gene expression analysis

Cell of origin (COO) determination on Lymph2Cx assay (Nanostring, Seattle, WA) was performed as previously published.[21] Gene expression levels of *MYC* and *ETS1* were investigated by real time quantitative PCR (**Online Supplementary Methods)** using Taqman assays described in **Online Supplementary Table S4**.

Statistical methods

The $\chi 2$ method was used for categorical variables and Student's t-test for continuous variables. Non-parametric tests were applied when necessary. The P-values for multiple comparisons were adjusted using the Benjamini–Hochberg correction. Survival curves were estimated by Kaplan-Meier method. Statistical analyses were carried out with SPSS v22 and R software v3.1.3.

Results

Identification of BLL-11q cases

To identify BLL-11q cases we reevaluated the presence of *MYC* translocation in 95 cases diagnosed as BL, atypical BL or HGBCL, NOS. We confirmed the presence of *MYC* rearrangements in 78 cases (82.1%), from which 67 (70.5%) were classified as BL. Since the 11q aberration has been found mainly in children and young adult (<40 year-old) patients,[4] we analyzed separately the 60 patients under 40 years and the 35 older patients (**Online Supplementary Figure S1**).

In the younger cohort (n=60), the 46 (76.7%) cases with *MYC* translocation were classified as BL. To find BLL-11q cases, we initially used the Oncoscan platform in the remaining 14 *MYC*-negative patients and detected the presence of the 11q gain/loss alteration in eight of those. Additionally, we found a CN pattern consistent with the presence of 11q alteration in 3 recent consultation cases from SEHOP (**Online Supplementary Figures S1 and S2**). Then, among those BLL-11q cases we could verify the presence of the 11q aberration by FISH in all 10 evaluable cases (**Online Supplementary Figure S3 and Supplementary Table S5**). Morphological, clinical, genetic features and consensus diagnosis of the 11 BLL-11q identified in our files are summarized in **Table 1**. The 6 cases negative for the *MYC* rearrangement and 11q aberrations by Oncoscan were re-classified as DLBCL (3 cases) or HGBCL, NOS (3 cases). The DLBCL had predominant centroblastic morphology, germinal center phenotype, very high proliferative index and focal “starry sky” pattern (**see Online Supplementary Results**). The absence of 11q alterations was also verified using the 11q FISH probe in 4 of these *MYC*/11q negative cases with evaluable material (**Online Supplementary Figure S1A**).

In the 35 older (≥ 40 yr) patients, a *MYC* translocation was found in 32 cases; 1 was classified as DLBCL, 21 as BL, and 10 were HGBCL with double or triple hit (*BCL2*

and/or *BCL6* translocations). Only 3 cases were negative for *MYC* translocations and were classified as HGBCL, NOS (**Online Supplementary Figure S1B and supplementary Results**). We screened these cases with the 11q FISH probe and the 3 were negative for the 11q aberration.

Clinical and morphological results of BLL-11q cases

The 11 patients with BLL-11q had a mean age of 15 years (range 8-37); eight were male (**Table 1**). Eight tumors were reclassified morphologically as HGBCL, NOS, two as DLBCL and only one case was considered atypical BL. None of the cases were considered as typical BL (**Figure 1**). Six cases exhibited starry sky pattern and two had a nodular growth pattern with the presence of a disrupted follicular dendritic cell meshwork (**Figure 1C**). Ki67 was very high in all the samples, similar to BL. All cases had a germinal center (GC) phenotype and GCB signature by Nanostring Lymph2Cx assay. MUM1/IRF4 was negative in all 11 cases. One case expressed BCL2 (**Figure 1D**). LMO2, a germinal center marker that is usually seen in GCB-DLBCL but not in BL[18] was expressed in 5 cases (**Figure 1A-B**). Interestingly, using a 40% cut off,[19] 5 cases were positive for MYC expression. However, only one case showed a diffuse and intense positivity meanwhile the other four cases had either only positivity in around 50% of the cells or the intensity was not the expected in typical BL. Additionally, *MYC* RNA levels were significantly lower in BLL-11q than in *MYC*-positive BL (relative expression 0.07 *vs* 0.36, *P*=0.019) (**Online Supplementary Figure S4A**). The Epstein-Barr virus hybridization (EBER) was negative in the nine cases tested.

Clinically, BLL-11q had frequent nodal localized presentation (8/11) in the head and neck region. Two cases had an extranodal presentation, one in the context of an acute appendicitis and the other debuted as an omental mass. Eight patients (73%) had stage I-II, and one patient presented in an advanced stage (IVAE) with widespread disease in the context of chronic HIV infection. All cases were treated with

chemotherapy, including Rituximab in five. All patients were alive with no disease after median follow-up of 30 months (**Table 1**).

Copy number analysis

The CN analysis of all the 11 BLL-11q cases showed a total of 78 alterations (Mean 7.1; Range 2-15) (**Online Supplementary Table S5 and S6**). Seven cases had the typical 11q gain/loss pattern (**Figure 2A-B, Online Supplementary Figure S2**), two cases had only an 11q terminal deletion, one case showed a complex 11q alteration with two gains and two losses, and finally one case had an 11q23.3-q25 copy number neutral loss of heterozygosity (CNN-LOH) in addition to gain (**Online Supplementary Figure S2**). Two minimal regions of gain were identified (chr11:103326831-111737912/11q22.3-q23.1 and chr11:114767237-116764582/11q23.3) whereas the minimal region of loss was depicted in chr11:128214400-132020453/11q24.3-q25 (Including *ETS1* and *FLI1* genes). No cases with homozygous deletions of these two targets were observed in our series. The breakpoint region between gain and loss was not conserved and span from chr11:118352769 to chr11:121062860. Amplification in the 11q arm were observed in four cases, with a minimal region chr11:118347020-120155799/11q23.3, including *USP2* gene (**Online Supplementary Figure S5**). The most recurrent CNA other than 11q were 12q12-q21.1 gains and 6q12.1-q21 losses (**Figure 2A**).

BLL-11q cases displayed similar levels of complexity than *MYC*-positive BL (7.1 *vs* 6 alterations),[20] but significantly lower than GCB-DLBCL (7.1 *vs* 19, $P<0.0001$).[13] The BLL-11q genomic profile differed from that of BL and DLBCL (**Online Supplementary Figure S6**). BLL-11q had frequent gains of 5q21.3-q32 and losses of 6q12.1-q21 and lacked the 1q gains seen in *MYC*-positive BL. BLL-11q also lacked alterations typically seen in GCB-DLBCL such as gains of 2p16.1 and 7p and losses of 1p36.32.

The six tumors negative for both *MYC* and 11q-aberrations in patients younger than 40 years had similar levels of genomic complexity than those observed in BLL-11q (7.01 vs 11.83; *P*=0.16) (**Online Supplementary Figure S7A**). The unique significant aberration that distinguished the two groups was the presence/absence of the 11q aberration.

The review of the literature regarding other lymphoid neoplasms confirmed that the 11q alteration observed in BLL-11q is mainly absent in other lymphoma entities with the exception of transformed follicular lymphoma (16%) (**Online Supplementary Results**).[22]

NGS and gene expression analysis

Target NGS showed a total of 49 potential driver mutations affecting 27 different genes (mean=4.9 mutations per case) (**Figure 2C-D**, **Online Supplementary Figures S8 and S9; Online Supplementary Table S7**). Interestingly, all cases lacked the typical BL mutations in *ID3*, *TCF3*, or *CCND3* genes, and their mutational profile was more similar to that of other GC derived lymphomas with recurrent mutations affecting *BTG2* (4 cases), *DDX3X, ETS1, EP300,* and *GNA13* (3 cases each) (**Online Supplementary Table S8**). Five cases had mutations in epigenetic modifiers genes such as *EP300*, *CREBBP*, *KMT2C*, *EZH2*, *ARID1A*, *KMT2D, HIST1H1D* and *HIST1H2BC*. Two cases had concomitant *TMEM30A* deleterious mutations associated with 6q14.1 deletion as seen in DLBCL but not in BL (**Figure 2C**).[14-16]

BTG2 mutations found in 4 cases were 3 missense and 1 deletion in a splicing site. *BTG2* is a tumor suppressor gene with an important role in G1/S transition through inhibition of CCND1 in a pRb-dependent mechanism.[23] These *BTG2* inactivating mutations could release CCND1 inhibition and accelerate G1/S transition. *GNA13* mutations were found in 3 cases including 4 missense, 2 nonsense, and 1 missense mutation in a splicing site. Two *MYC* missense mutations occurred in the central

domain of the protein, but did not affect threonine phosphorylation sites (**Online Supplementary Table S7**).[24] *ETS1* mutations have been previously described in BLL-11q and ABC-DLBCL[13,17] but not in conventional BL (**Online Supplementary Table S8**).[14,15] We detected 3 coding mutations located on the winged helix-turn-helix DNA-binding domain but the previously described exon 1 mutations (NM_005238) were absent in this series. *ETS1* RNA expression was lower in BLL-11q than *MYC*-positive BL (relative expression 6.6 *vs* 19.3, $p < .001$) and was also lower in *ETS1* mutated than wild-type BLL-11q (relative expression 1.9 *vs* 8.6, $P=0.03$) (**Online Supplementary Figure S4B**).

The mutational profile of 4 *MYC*-negative/11q alteration-negative cases with material available was analyzed using the same approach. No mutations in *BTG2, EP300* or *ETS1* genes were observed. Moreover, three out of four did not harbor any BL-related mutation on *ID3, TCF3* and *CCND3* whereas the fourth case had a mutational profile commonly seen in BL with *MYC, DDX3X, SMARC4, CCND3* and *TP53* mutations (**Online Supplementary Figure S7B**).

Discussion

BLL-11q was initially recognized as a particular subset of HGBCL that had an expression profile and some pathological characteristics similar to BL but lacked *MYC*-translocations and alternatively shared a common pattern of gains at 11q23 associated with losses at 11q24-qter. The particular features of these cases raise some uncertainty on their precise categorization as a variant of BL or a tumor related to other HGBCL.[1,4-6,9-11] On the other hand, the limited number of cases reported and the different methodologies used for their recognition do not provide a clear view of their incidence and clinico-pathological characteristics.

In this study we have searched our files for cases that could be reclassified as BLL-11q among 95 tumors previously classified as BL, atypical BL, or HGBCL, NOS and found 8 (8%) cases with the chromosomal aberration. These cases together with 3 additional cases received on consultation were investigated for the copy number alteration CNA and mutational profiles and compared to the genomic aberrations recently identified in BL, DLBCL, and HGBCL.[13-17] BLL-11q had similar levels of complexity as *MYC*-positive BL,[20] but significantly lower than GCB-DLBCL.[13] The BLL-11q genomic profile differed from that of BL and DLBCL (**Online Supplementary Figure S6**). BLL-11q had frequent gains of 5q21.3-q32 and losses of 6q12.1-q21 and lacked the 1q gains seen in *MYC*-positive BL. BLL-11q also lacked alterations typically seen in GCB-DLBCL such as gains of 2p16.1 and 7p and losses of 1p36.32. Additionally, we identified a mutational profile in BLL-11q different from that of *MYC*-positive BL since all cases lacked the typical BL mutations in *ID3*, *TCF3*, or *CCND3* genes and had mutations in *BTG2*, *DDX3X, ETS1* not seen in BL. In addition, BLL-11q had mutations in epigenetic modifier genes such as *EP300*, *CREBBP*, *KMT2C*, *EZH2*, *ARID1A*, *KMT2D, HIST1H1D* and *HIST1H2BC* that are common in DLBCL, particularly of the GC subtype. Other genes frequently mutated in GC-DLBCL but not in BL were *GNA13* and *TMEM30A* associated with 6q14.1.[14-16]

We also compared our results with two recent studies on HGBCL (including double and triple hit lymphomas).[25,26] These cases have also recurrent mutations on histone modifier genes such as *KMT2D*, *CREBBP* or *EZH2* (**Online Supplementary Table S8**). Intriguingly, HGBCL, NOS, mainly with *MYC*-translocations, shared mutations in genes frequently mutated in both BL and GC-DLBCL.[25,26] All these observations suggest that BLL-11q is a neoplasm closer to other GC-derived lymphomas rather than BL in which the 11q aberration together with other mutations may play a relevant role in their pathogenesis. Whereas this manuscript was on revision, Wagener et al published a mutational study of 15 BLL-11q. Similar to our findings, no mutations in *ID3/TCF3* were found and those cases carried frequent mutations in GC-DLBCL associated genes such as *GNA13*, *FOXO1* and *EZH2*. Intriguingly, this study did not find mutations in *BTG2*, *KMT2D*, *KMT2C* or *CREBBP* observed in our study.[27] All together these findings indicate that the genomic and mutational profile of BLL-11q is different from those of BL and more similar to other GC derived lymphomas.

In addition to the genetic differences, our BLL-11q differed clinically, morphologically and phenotypically from conventional BL and instead showed features more consistent with HGCBL or DLBCL. As in previous studies, all our patients were younger than 40 years, although occasional cases in older patients have been reported.[4,5,27] Contrary to BL, BLL-11q presented with localized lymphadenopathy in most of our cases.[4,5,27] These cases have a favorable outcome after therapy, although the optimal clinical management remains to be determined. Morphologically, our cases had a prominent "starry sky" pattern and high proliferation (>90%) but did not have the typical cytological features of BL since they were better classified as HGBCL with blastoid or intermediate features between HGBCL (8 cases) and DLBCL (2 cases) and only one had features of atypical BL. As previously reported,[4] two of our cases displayed a follicular growth pattern, with an underlying meshwork of follicular dendritic cells, raising the differential

diagnosis with other pediatric lymphomas such as large B-cell lymphoma with *IRF4* rearrangement.[3] However, BLL-11q do not express IRF4/MUM1 and frequently exhibited a starry sky pattern with frequent mitotic figures, features that are not usual in large B-cell lymphoma with *IRF4* rearrangement. We also identified different immunohistochemical stainings that could help in the differential diagnosis with other lymphomas entities. LMO2, a germinal center marker that is typically downregulated in BL and other lymphomas with *MYC* translocation,[18] is detected in 46% of our BLL-11q. In addition, and contrary to BL, MYC expression with a diffuse and intense pattern was only detected in one of our cases while the other four positive cases either exhibited partial positivity or the intensity was weak contrary to the pattern seen in BL.

The negativity for *MYC* rearrangement is a crucial element for the recognition of these cases. The recommended technique for interrogating *MYC* translocations in the clinical practice is the FISH analysis using break-apart probes, with the limitation that a subset of 4% of *MYC* positive cases are not detected with this method but picked up using *MYC*/IGH probes.[28] The genetic feature that distinguishes BLL-11q is an alteration of the 11q arm that prototypically is characterized by an 11q23.2-q23.3 gain/amplification and 11q24.1-qter loss. Additionally, isolated cases have been recognized with single 11q24.1-qter terminal loss or 11q23 gain with 11q24 CNN-LOH.[4,11] In our study we have identified the presence of these 11q alterations using CN array. We also confirmed the presence of 11q alterations by FISH analysis with a custom probe in all tested cases, suggesting that this approach may be useful in the clinical practice to identify these cases (**Online Supplementary Table S8**). The specificity of this FISH approach was also confirmed by the fact that no false positive cases were observed in the 12 lymphoma cases in which the array showed a normal 11q pattern. Nevertheless, more studies on the clinical value of this probe are needed and, for the time being, confirmation of the finding by CN array would be desirable. The specific 11q alteration observed in BLL-11q should be distinguished from other 11q aberrations such as 11q

gains of the 11q24 region that include *ETS1* and *FLI1* detected in DLBCL [29] or the 11q25 losses missing *ETS1* and *FLI1* described in some post-transplant lymphoproliferative disorders.[30,31] On the other hand, although the 11q23 gain/11q24-qter loss of BLL-11q is mainly absent in other lymphoma entities, its detection should not be considered as a unique tool to diagnose BLL-11q cases since some transformed FL may carry a similar 11q aberration pattern.[22]

In summary, BLL-11q is a germinal center derived lymphoma with a genomic and mutational profile closer to HGBCL or GC-DLBCL rather than BL in which the 11q aberration, together with other mutations, may play a relevant role in their pathogenesis. These observations support a reconsideration of the "Burkitt-like" term for these tumors. Although, the most appropriate name is not easy to propose and requires broader discussion and consensus, we think that the term "aggressive B-cell lymphoma with 11q aberration" captures their pathological features. To identify these cases we suggest performing CN arrays or FISH with the 11q probe in cases with BL, DLBCL, and HGBCL morphology, germinal center phenotype and very high proliferative index (>90%), without *MYC* rearrangements, in young patients. The recognition of these tumors is clinically relevant because they have a favorable outcome after therapy, although further studies are needed to determine the optimal clinical management.

References

1. Swerdlow SH, Campo E, Harris NL, Jaffe ES, Pileri SA, Stein H, Thiele J (Eds) WHO Classification of Tumours of Haematopoietic and Lymphoid Tissues. (Revised 4th edition) IARC: Lyon 2017.

2. Schmidt J, Gong S, Marafioti T, et al. Genome-wide analysis of pediatric-type follicular lymphoma reveals low genetic complexity and recurrent alterations of TNFRSF14 gene. Blood. 2016;128(8):1101-1111.

3. Salaverria I, Philipp C, Oschlies I, et al. Translocations activating IRF4 identify a subtype of germinal center-derived B-cell lymphoma affecting predominantly children and young adults. Blood. 2011;118(1):139-147.

4. Salaverria I, Martin-Guerrero I, Wagener R, et al. A recurrent 11q aberration pattern characterizes a subset of MYC-negative high-grade B-cell lymphomas resembling Burkitt lymphoma. Blood. 2014;123(8):1187-1198.

5. Rymkiewicz G, Grygalewicz B, Chechlinska M, et al. A comprehensive flow-cytometry-based immunophenotypic characterization of Burkitt-like lymphoma with 11q aberration. Mod Pathol. 2018;31(5):732-743.

6. Ferreiro JF, Morscio J, Dierickx D, et al. Post-transplant molecularly defined Burkitt lymphomas are frequently MYC-negative and characterized by the 11q-gain/loss pattern. Haematologica. 2015;100(7):e275-e279.

7. Capello D, Scandurra M, Poretti G, et al. Genome wide DNA-profiling of HIV-related B-cell lymphomas. Br J Haematol. 2010;148(2):245-255.

8. Deffenbacher KE, Iqbal J, Liu Z, Fu K, Chan WC. Recurrent chromosomal alterations in molecularly classified AIDS-related lymphomas: an integrated analysis of DNA copy number and gene expression. J Acquir Immune Defic Syndr. 2010;54(1):18-26.

9. Poirel HA, Cairo MS, Heerema NA, et al. Specific cytogenetic abnormalities are associated with a significantly inferior outcome in children and adolescents with mature B-cell non-Hodgkin's lymphoma: results of the FAB/LMB 96 international study. Leukemia. 2009;23(2):323-331.

10. Havelange V, Ameye G, Theate I, et al. The peculiar 11q-gain/loss aberration reported in a subset of MYC-negative high-grade B-cell lymphomas can also occur in a MYC-rearranged lymphoma. Cancer Genet. 2016;209(3):117-118.

11. Grygalewicz B, Woroniecka R, Rymkiewicz G, et al. The 11q-Gain/Loss Aberration Occurs Recurrently in MYC-Negative Burkitt-like Lymphoma With 11q Aberration, as Well as MYC-Positive Burkitt Lymphoma and MYC-Positive High-Grade B-Cell Lymphoma, NOS. Am J Clin Pathol. 2017;149(1):17-28.

12. Dunleavy K, Gross TG. Management of aggressive B-cell NHLs in the AYA population: an adult vs pediatric perspective. Blood. 2018;132(4):369-375.

13. Karube K, Enjuanes A, Dlouhy I, et al. Integrating genomic alterations in diffuse large B-cell lymphoma identifies new relevant pathways and potential therapeutic targets. Leukemia. 2018;32(3):675-684.

14. Richter J, Schlesner M, Hoffmann S, et al. Recurrent mutation of the ID3 gene in Burkitt lymphoma identified by integrated genome, exome and transcriptome sequencing. Nat Genet. 2012;44(12):1316-1320.

15. Schmitz R, Young RM, Ceribelli M, et al. Burkitt lymphoma pathogenesis and therapeutic targets from structural and functional genomics. Nature. 2012;490(7418):116-120.

16. Love C, Sun Z, Jima D, et al. The genetic landscape of mutations in Burkitt lymphoma. Nat Genet. 2012;44(12):1321-1325.

17. Morin RD, Mungall K, Pleasance E, et al. Mutational and structural analysis of diffuse large B-cell lymphoma using whole-genome sequencing. Blood. 2013;122(7):1256-1265.

18. Colomo L, Vazquez I, Papaleo N, et al. LMO2-negative Expression Predicts the Presence of MYC Translocations in Aggressive B-Cell Lymphomas. Am J Surg Pathol. 2017;41(7):877-886.

19. Johnson NA, Slack GW, Savage KJ, et al. Concurrent expression of MYC and BCL2 in diffuse large B-cell lymphoma treated with rituximab plus cyclophosphamide, doxorubicin, vincristine, and prednisone. J Clin Oncol. 2012;30(28):3452-3459.

20. Scholtysik R, Kreuz M, Klapper W, et al. Detection of genomic aberrations in molecularly defined Burkitt's lymphoma by array-based, high resolution, single nucleotide polymorphism analysis. Haematologica. 2010;95(12):2047-2055.

21. Scott DW, Wright GW, Williams PM, et al. Determining cell-of-origin subtypes of diffuse large B-cell lymphoma using gene expression in formalin-fixed paraffin-embedded tissue. Blood. 2014;123(8):1214-1217.

22. Bouska A, McKeithan TW, Deffenbacher KE, et al. Genome-wide copy-number analyses reveal genomic abnormalities involved in transformation of follicular lymphoma. Blood. 2014;123(11):1681-1690.

23. Guardavaccaro D, Corrente G, Covone F, et al. Arrest of G(1)-S progression by the p53-inducible gene PC3 is Rb dependent and relies on the inhibition of cyclin D1 transcription. Mol Cell Biol. 2000;20(5):1797-1815.

24. Bahram F, von der LN, Cetinkaya C, Larsson LG. c-Myc hot spot mutations in lymphomas result in inefficient ubiquitination and decreased proteasome-mediated turnover. Blood. 2000;95(6):2104-2110.

25. Evrard SM, Pericart S, Grand D, et al. Targeted next generation sequencing reveals high mutation frequency of CREBBP, BCL2 and KMT2D in high-grade B-cell lymphoma with MYC and BCL2 and /or BCL6 rearrangements. Haematologica. 2018 Oct 11. [Epub ahead of print]

26. Momose S, Weissbach S, Pischimarov J, et al. The diagnostic gray zone between Burkitt lymphoma and diffuse large B-cell lymphoma is also a gray zone of the mutational spectrum. Leukemia. 2015;29(8):1789-1791.

27. Wagener R, Seufert J, Raimondi F, et al. The mutational landscape of Burkitt-like lymphoma with 11q aberration is distinct from that of Burkitt lymphoma. Blood. 2018 Dec 19. [Epub ahead of print]

28. King RL, McPhail ED, Meyer RG, et al. False-negative Rates for MYC FISH Probes in B-cell Neoplasms. Haematologica. 2018 Dec 6. [Epub ahead of print]

29. Bonetti P, Testoni M, Scandurra M, et al. Deregulation of ETS1 and FLI1 contributes to the pathogenesis of diffuse large B-cell lymphoma. Blood. 2013;122(13):2233-2241.

30. Rinaldi A, Kwee I, Poretti G, et al. Comparative genome-wide profiling of post-transplant lymphoproliferative disorders and diffuse large B-cell lymphomas. Br J Haematol. 2006;134(1):27-36.

31. Rinaldi A, Capello D, Scandurra M, et al. Single nucleotide polymorphism-arrays provide new insights in the pathogenesis of post-transplant diffuse large B-cell lymphoma. Br J Haematol. 2010;149(4):569-577.

Table 1. Pathological and clinical features of eleven Burkitt -like lymphoma with 11q aberration.

Case	Age/ gender	Biopsy Site	Original diagnosis	Final diagnosis	Immunophenotype					Stage*	COO Nanostring (Lymph2Cx)	Chemotherapy	Rituximab	Outcome/ follow-up
					CD10& BCL6	IRF4/ MUM1	BCL2	LMO2	MYC					
#1	27, M	Laterocervical LN	Atypical BL	HGBCL, NOS	+	-	-	-	+	I	GCB	A	Yes	CR, 72m
#2**	37,M	Axillary LN	Atypical BL	DLBCL	+	-	-	+	-	IV-E	GCB	A	Yes	CR, 112m
#3	8,F	Tonsil	HGBCL	DLBCL & HGBCL blastoid	+	-	-	-	-	II	GCB	P	No	CR, 54m
#4	17,F	Submaxilar LN	HGBCL	HGBCL, NOS	+	-	-	+	+	I	GCB	A	Yes	CR, 22m
#5	14,F	Laterocervical LN	HGBCL	HGBCL with features intermediate between BL and DLBCL	+	-	+	+	-	I	GCB	P	No	CR, 29m
#6	14,M	Appendix	HGBCL	DLBCL	+	-	-	+	-	II	GCB	P	No	CR, 25m
#7	8, M	Laterocervical LN	BL	Atypical BL	+	-	-	-	-	I	GCB	P	No	CR, 113m
#14	8,M	Laterocervical LN	BL	HGBCL blastoid	+	-	-	-	Weak +	II	GCB	P	No	CR, 15m
#15	12,M	Laterocervical mass	DLBCL	HGBCL, NOS	+	-	-	-	+	I	GCB	P	No	CR, 35m
#16	14, M	Laterocervical LN	DLBCL	HGBCL, NOS	+	-	-	+	-	III	GCB	P	Yes	CR, 12m
#17	16, M	Omentum	HGBCL	HGBCL, NOS	+	-	-	-	+	III	GCB	A	Yes	CR, 4m

Abbreviations: M: male; F: Female; LN: Lymph node; BL: Burkitt Lymphoma; HGBCL: High grade B-cell lymphoma; NOS: Not otherwise specified; DLBCL: Diffuse Large B-cell lymphoma; Epstein-Barr virus *in situ* hybridization (EBER) were negative in all 9 tested cases. E: extranodal; COO: Cell of origin; GCB: Germinal center B-cell; A: Adult schema protocol (R-CHOP or Burkimab); P: pediatric schema protocol. All patients received CNS prophylaxis

*Stage was established according St.Jude/International pediatric NHL staging system (IPNHLSS) or Ann Arbor staging system for pediatric and adult patients respectively.

**HIV positive.

Figure legends

Figure 1. Morphological features of Burkitt-like lymphoma with 11q aberration cases. (**A1-A3**) Case #2 shows typical DLBCL morphology with large and irregular cells resembling centroblasts. This case was positive for (**A2**) LMO2 and negative for (**A3**) MYC. (**B1-B3**) Case #4 corresponds to a tumor with HGBCL morphology. It is composed mostly medium-sized cells with mild heterogeneity. Notice the "starry sky" pattern. This case was positive for (**B2**) MYC and (**B3**) LMO2 expression. (**C1-C2**; case #7) Lymph node with nodular architecture and "starry sky" pattern with large follicles and disrupted follicular cell meshwork highlighted with (**C2**) CD21. (**D1-D2;** case #5) shows a case with HGBCL features with expression of (**D2**) BCL2 in the neoplastic cells.

Figure 2. Genetic features of Burkitt-like lymphoma with 11q aberration cases. (A) Global copy number profile of the 11 Burkitt-like lymphomas with 11q aberration. X-axis indicates chromosomes from 1 to Y and p to q. The vertical axis indicates frequency of the genomic aberration among the analyzed cases. Gains are depicted in blue, losses are depicted in red. **(B)** Individual CN profile of case #16 showing a prototypical, gain, loss and amplification in the 11q region. Each probe is aligned from chromosome 1 to Y and p to q arm. **(C)** Mutational overview of 10 BLL with 11q aberration. The heat map shows the case specific pattern of driver mutations found by next generation sequencing. Each column represents a case and each row represents a gene. The right bar graph illustrates the mutation frequency of each gene. **(D)** A diagram of the relative positions of driver mutations is shown for *BTG2*, *ETS1* and *GNA13* genes. Domains BTG2: BTG family domain. Domains ETS1: PNT: Pointed domain; TAD: transactivation domain; H-1/2: inhibitory α-helices 1/2; DBD: DNA binding domain; H4-5: α-helix 4/5. Domains GNA13: G-alpha: G protein alpha subunit. Circles indicate missense mutations, triangles indicate truncating mutations and rhombus indicate splicing mutations.

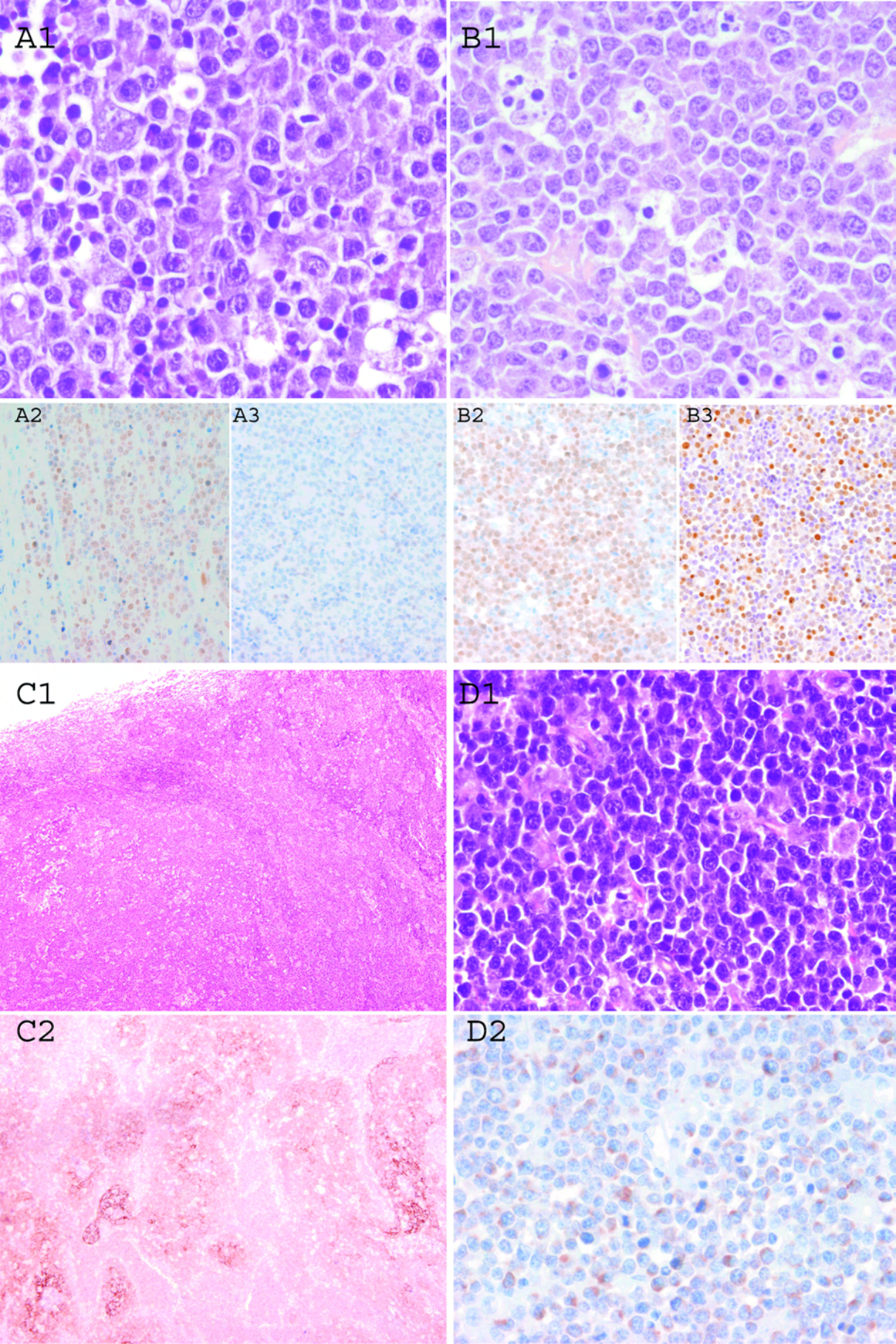
A1
B1
A2
A3
B2
B3
C1
D1
C2
D2

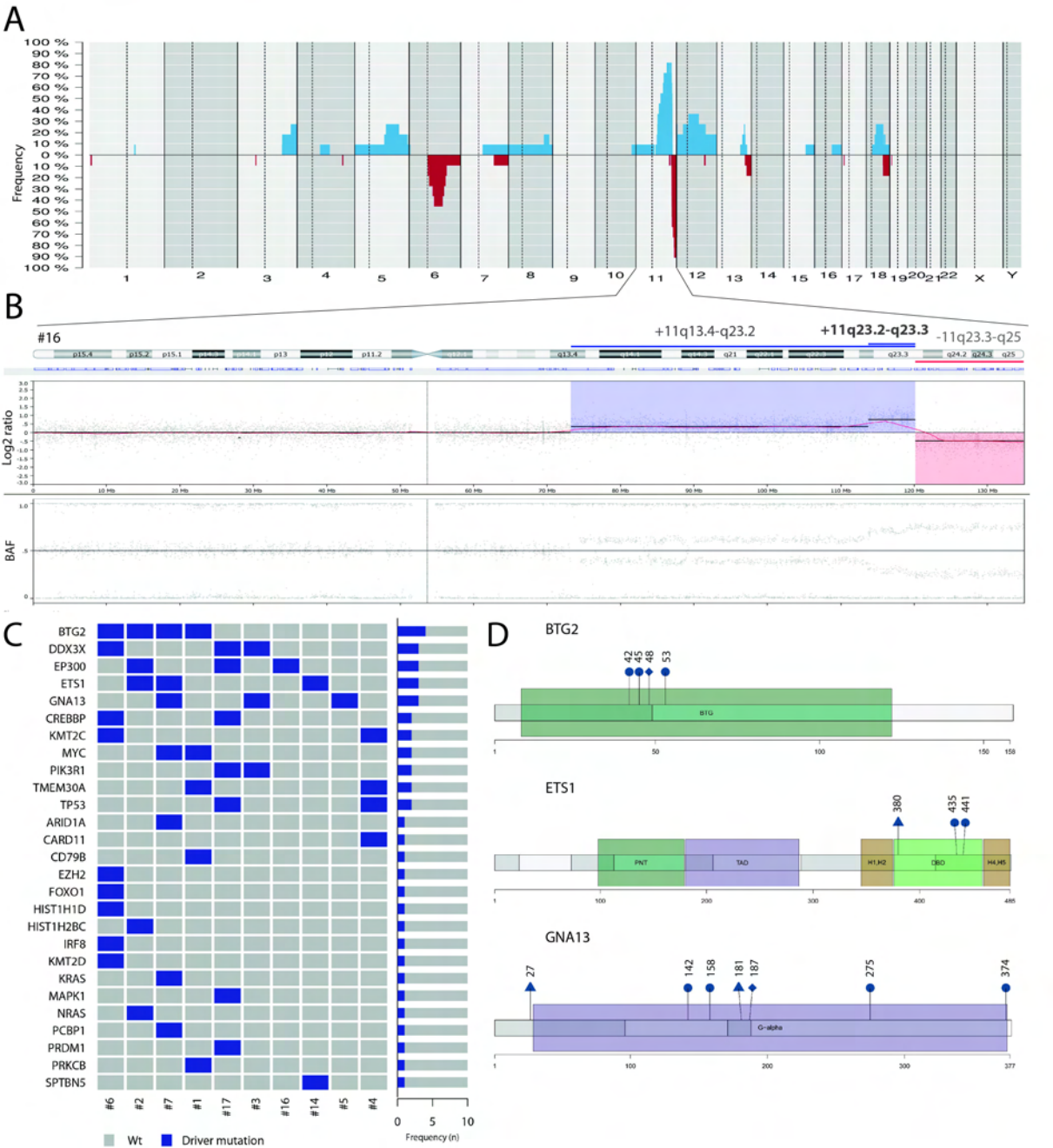
A
Frequency
100 %
90 %
80 %
70 %
60 %
50 %
40 %
30 %
20 %
10 %
0 %
1 2 3 4 5 6 7 8 9 10 11 12 13 14 15 16 17 18 19 20 21 22 X Y
B
#16
+11q13.4-q23.2
+11q23.2-q23.3
-11q23.3-q25
Log2 ratio
BAF
C
BTG2
DDX3X
EP300
ETS1
GNA13
CREBBP
KMT2C
MYC
PIK3R1
TMEM30A
TP53
ARID1A
CARD11
CD79B
EZH2
FOXO1
HIST1H1D
HIST1H2BC
IRF8
KMT2D
KRAS
MAPK1
NRAS
PCBP1
PRDM1
PRKCB
SPTBN5
#6 #2 #7 #1 #17 #3 #16 #14 #5 #4
0 5 10
Frequency (n)
Wt
Driver mutation
D
BTG2
42 45 48 53
BTG
ETS1
380
435 441
PNT
TAD
H1,H2
DBD
H4,H5
GNA13
27
142 158 181 187
275
374
G-alpha

Supplementary Material

Burkitt-like lymphoma with 11q aberration: A germinal center derived lymphoma genetically unrelated to Burkitt lymphoma

Gonzalez-Farre & Ramis-Zaldivar et al

Supplementary Methods

Copy number analysis

DNAs were hybridized on Oncoscan FFPE or SNP array platform (ThermoFisher Scientific, Waltham, MA). Gains and losses and copy-number neutral loss of heterozygosity (CNN-LOH) regions were evaluated and visually inspected using Nexus Biodiscovery version 9.0 software (Biodiscovery, Hawthorne, CA). Human reference genome was GRCh37/hg19. The copy number alterations (CNAs) with minimum size of 100 kb and CNN-LOH larger than 5 Mb were considered informative. Physiological deletions of the immunoglobulin loci were excluded from the analysis. T-cell receptor locus deletions were also excluded, most probably representing physiological deletions of accompanying reactive T cells. Copy number data are deposited at GEO database GSE116527. Published CN data on *MYC*-positive BL[1] were reanalyzed.

Library preparation SureSelect XT and Targeted sequencing approach

DNA and RNA were extracted using standard protocols from formalin fixed paraffin embedded material in 12 and frozen tissue in 3 cases (Qiagen, Hilden, Germany). A total of 100ng of genomic DNA was sheared using the Covaris S220 focused-ultra sonicator (Covaris, Woburn, MA) to a target peak size of 150–200 bp. Library preparation were performed using SureSelectXT Custom Capture Library baits as described in SureSelectXT Target Enrichment System protocol (Agilent Technologies, Santa Clara, CA). For amplification of the post capture libraries, 10 to 13 cycles were performed depending on the initial sample quality. The libraries were qualified using the Bioanalyzer HS (Agilent technologies), quantified with the KAPA Library Quantification Kit (Kapa Biosystems, Wilmington, Massachusetts) and sequenced in a MiSeq instrument (Illumina, San Diego, CA) in a paired-end run of 150 bp. The average sequencing coverage of 10 Burkitt-like lymphoma with 11q (BLL-11q) cases across

regions was 478x (range 97-1229) and over 93% of the targeted regions were covered by at least 100 reads. (**Supplementary Figure S7**).

FASTQ files were generated by MiSeq control software and quality control of the raw data was performed using the FastQC tool (https://www.bioinformatics.babraham.ac.uk/projects/fastqc/). Sequencing reads were subsequently aligned to the human reference genome (GRCh37/hg19) using the Burrows-Wheeler Aligner–MEM algorithm.[2] Variant calling was performed using two different variant callers: Somatic Variant Caller (Illumina) and annotated using the VariantStudio software v3.0 and Mutect2 (Genome Analysis Toolkit (GATK), version 4.0.3)[3] and annotated by ANNOVAR.[4] We used Somatic Variant Caller (Illumina) with the default settings to analyze sequencing results and to call the variants. Low quality or low coverage calls (total depth <20) were excluded. For Mutect2 variants, low quality variants were also excluded using FilterMutectCalls (GATK) with default thresholds. Only variants identified by both algorithms were considered. For further analysis we excluded all synonymous and intron variants outside splicing sites (not included in the panel, with exception of intron 1 of *MYC*) and known polymorphisms described in the Single Nucleotide Polymorphism Database (dbSNP138) or ExAC database (release 2015) with more than 0.1% frequency according to the corresponding ethnicity. Finally, each variant was also inspected with the Integrative Genomics Viewer (IGV, Broad Institute, version 2.3) software to exclude artifacts.

Prediction of mutation effect

Since there was no germline DNA available, in order to select somatic variants, potential driver mutations were predicted according to previously published criteria[5] in which the 90% of the mutations classified as functional were demonstrated to be somatic **(Supplementary Table S7)**. Inclusion criteria were: 1) any variant described previously as somatic or functional on previous reports or COSMIC, 2) All truncating variants (nonsense, frameshift, splice donor or acceptor mutations; and 3) the

remaining missense variants that were predicted to be functionally deleterious using Mutation Assessor[6] and SIFT[7] predictors. Other predictors as Polyphen-2 (Polymorphism Phenotyping-2)[8] and CADD (Combined Annotation Dependent Depletion)[9] were also used.

Quantitative PCR

Gene expression levels of *MYC* and *ETS1* of 10 BLL-11q with RNA available and 12 conventional *MYC*-positive BL were investigated by real time quantitative PCR (qPCR) as described previously.[10] Complementary DNA synthesis was carried out from 500 ng of total RNA and the product was amplified and quantified using TaqMan Universal PCR Master Mix no AmpErase UNG (Thermo Fisher Scientific Inc.), designed primer sets, and TaqMan Gene Expression Assays for *MYC* (Hs00153408_m1) and *ETS1* (Hs00428293_m1) (Thermo Fisher Scientific Inc.).

DNA was analyzed using duplicates in a StepOne Plus Real-Time PCR System (Thermo Fisher Scientific Inc.). Relative quantification of gene expression was then analyzed with the $2^{-\Delta\Delta Ct}$ method using *B2M* (Hs00939627_m1), as the endogenous control gene, and Universal Human Reference RNA (Stratagene, Agilent Technologies, Santa Clara, CA, USA), composed of total RNA from 10 human cell lines, as the mathematical calibrator.

Supplementary Results

Morphological features of 9 *MYC*-negative, 11q-negative lymphoma cases

Among the 95 cases with an initial diagnosis of BL, atypical BL or high grade B-cell lymphoma, not otherwise specified (HGBCL,NOS) nine (9.5%) were negative for *MYC* rearrangements, using both the break-apart and the double fusion probes (only seven cases analyzed), and for the 11q alteration. After the morphological review three cases were better reclassified to diffuse large B-cell lymphoma (DLBCL). These cases were composed of a proliferation of centroblastic cells with starry sky pattern, germinal

center phenotype and very high proliferative index. One case was weakly positive for BCL2. The remaining 6 cases had HGBCL, NOS morphology, two of them with blastoid features. Four cases had a germinal center phenotype and BCL2 negativity and two cases had an activated phenotype with BCL2 positivity. All cases had a proliferative index close to 100%.

Comparison of Copy number profile of BLL-11q with other lymphoma entities

BLL-11q lymphoma had similar levels of genomic complexity as conventional *MYC*-positive BL with 7.1 vs. 6 alterations, respectively. However, gains of 5q21.3-q32 and losses of 6q12.1-q21 were virtually exclusive of BLL-11q whereas 1q gains were only seen in *MYC*-positive BL. In comparison to the two molecular DLBCL subtypes, BLL-11q cases displayed significantly lower levels of complexity than ABC and GCB-DLBCL (7.1 vs. 22 alterations in ABC and 19 alterations in GCB; both $P<0.001$), had the specific 11q alterations and lacked gains of 2p16.1 and 7p and losses of 1p36.32 associated with GCB phenotype and losses of 6q23.3, 9p21.3 and 17p13.2 related to ABC-DLBCL.

To determine the specificity of the 11q-gain/loss pattern in BLL-11q in comparison to lymphoid neoplasms other than BL and DLBCL, we screened previously published data considering both patterns of prototypical pattern of gain followed by loss or only the presence of terminal 11q24.3-q25 loss. Frequencies observed were less than 1% in all the reviewed entities including follicular lymphoma,[11] nodal marginal zone lymphoma,[12] chronic lymphocytic leukemia[13] or plasma cell myeloma[14,15] with exception of transformed follicular lymphoma[11] in which 16% cases, presented the 11q aberrations. These data suggest that this alteration is mainly absent in other recognized lymphoma entities and characterizes genetically BLL-11q tumors.

Supplementary Figures

Supplementary Figure S1. Diagram of the strategy used for the identification of Burkitt-like with 11q aberration in a cohort of **(A)** 60 patients <40 years old and **(B)** 35 patients ≥ 40 years old with a morphological diagnosis of Burkitt lymphoma (BL)/atypical BL and high grade B-cell lymphoma, not otherwise specified (HGBCL, NOS) according to the updated WHO Classification 2016.[16] Seven out of nine cases negative for both *MYC* and 11q alterations with material available were tested by MYC/IGH double color double fusion probe, and all resulted to be negative for the fusion. Abbreviations: DLBCL, diffuse large B-cell lymphoma; DHL, double hit lymphoma; THL, triple hit lymphoma.

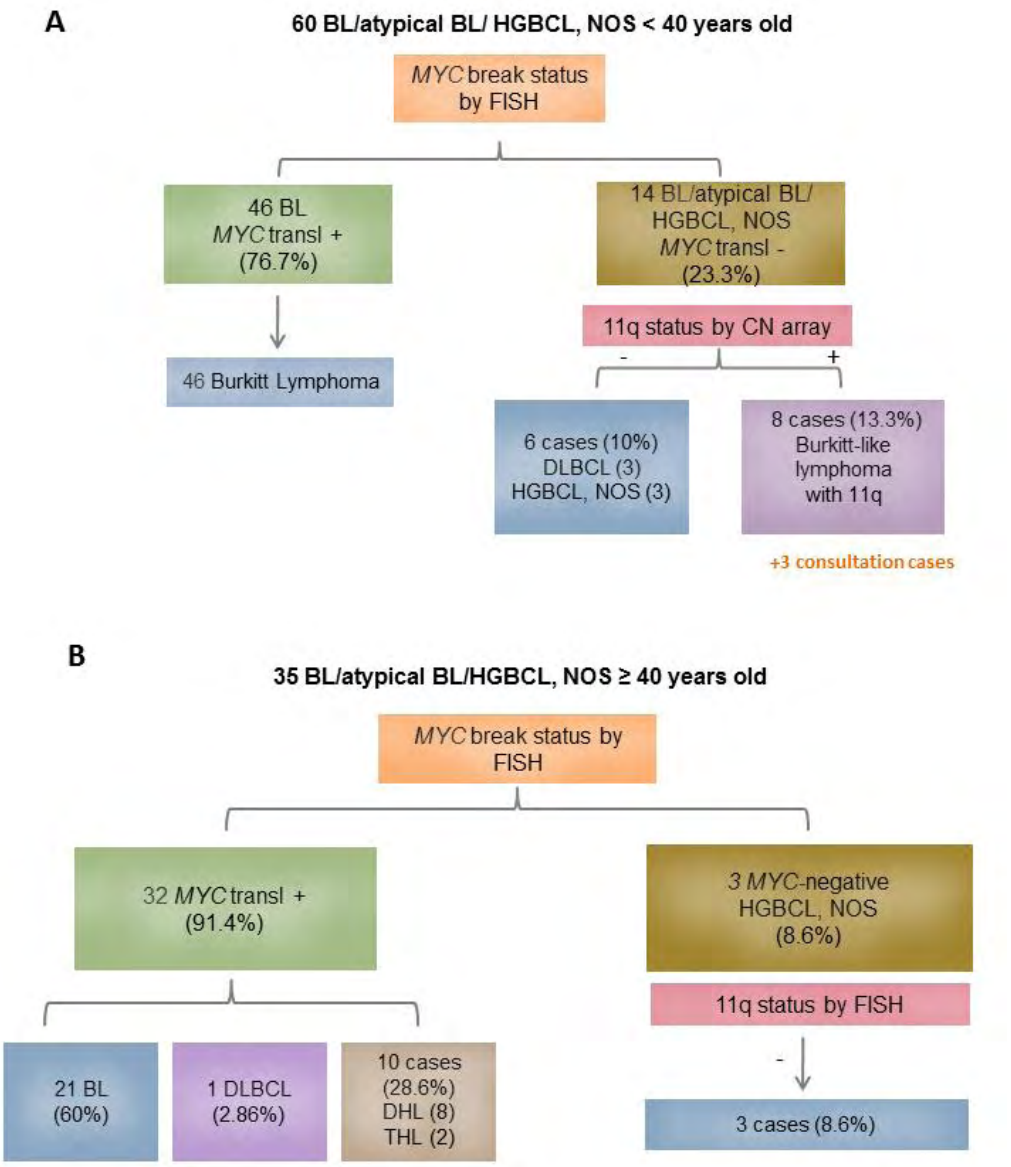

.

Supplementary Figure S2. Individual and integrative copy number plots of (A) eleven Burkitt-like with 11q and **(B)** six *MYC*-negative 11q-negative lymphoma cases. The vertical axis indicates frequency of the genomic aberration among the analyzed cases. Gains are depicted in blue, losses are depicted in red, and regions of CNN-LOH are represented in yellow.

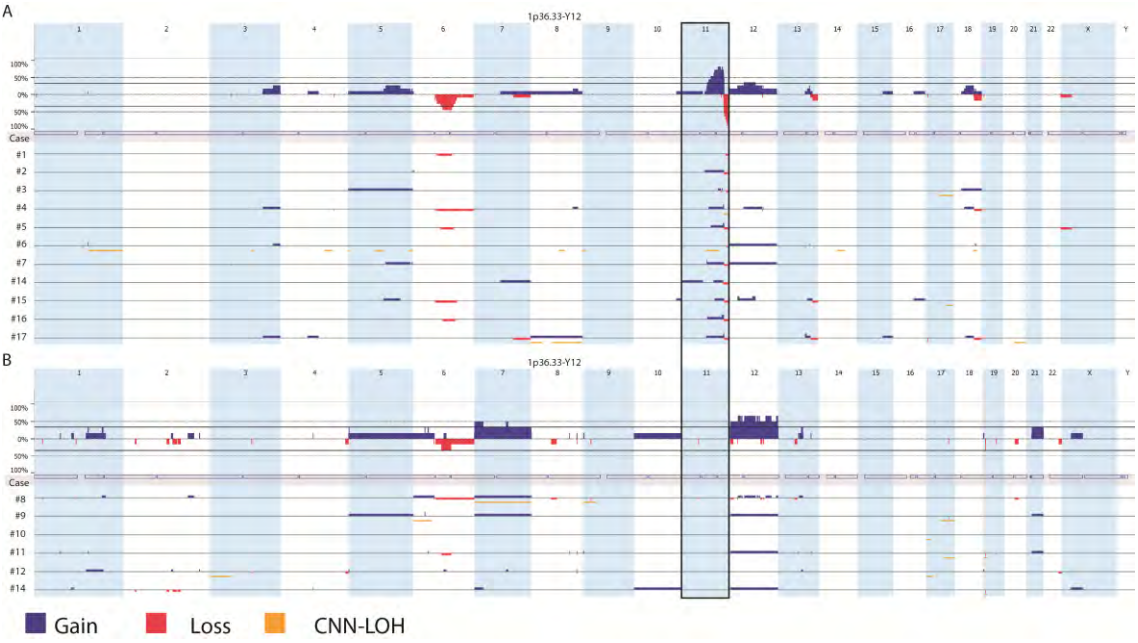

Supplementary Figure S3. Representative 11q aberration by FISH. (A) FISH image of a representative case (#17) harboring 11q aberration using a custom probe combining CEP11 (Spectrum Aqua), RP11-414G21 (Spectrum Green) and R11-629A20 (Spectrum Red) bac clones. **(B)** Two blue signals are observed per cell corresponding to the two chr11 centromeres, **(C)** the presence of three green signals per cell indicates 11q gain and **(D)** the presence of only one red is indicative of the 11q terminal loss.

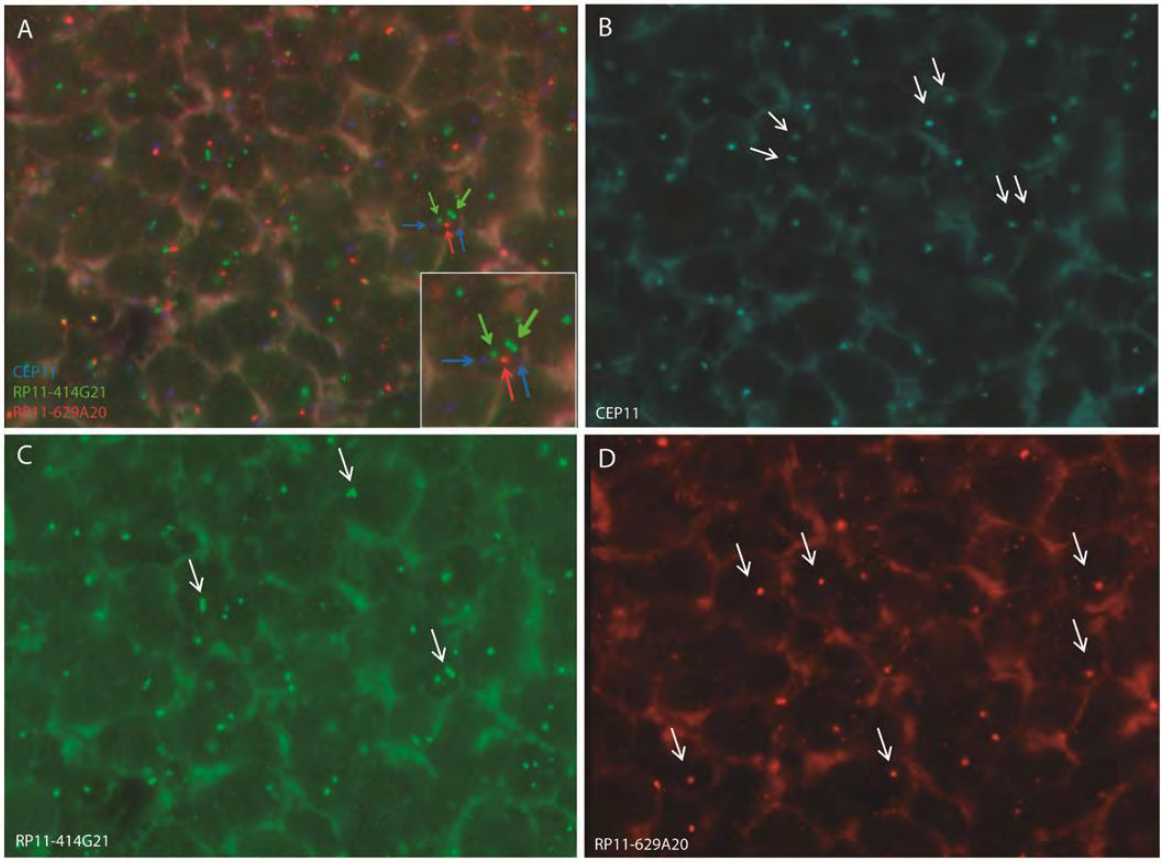

Supplementary Figure S4. *MYC* and *ETS1* RNA expression levels in BLL-11q. **(A)** Box plot of the percentage of *MYC* expression analyzed by qPCR in BLL-11q (n=9) vs. *MYC*-positive BL (n=9). **(B)** Box plot of the percentage of *ETS1* expression analyzed by qPCR in BLL-11q (n=10) vs. *MYC*-positive BL (n=12). The significance of difference was determined by t-test and Mann-Whitney test respectively.

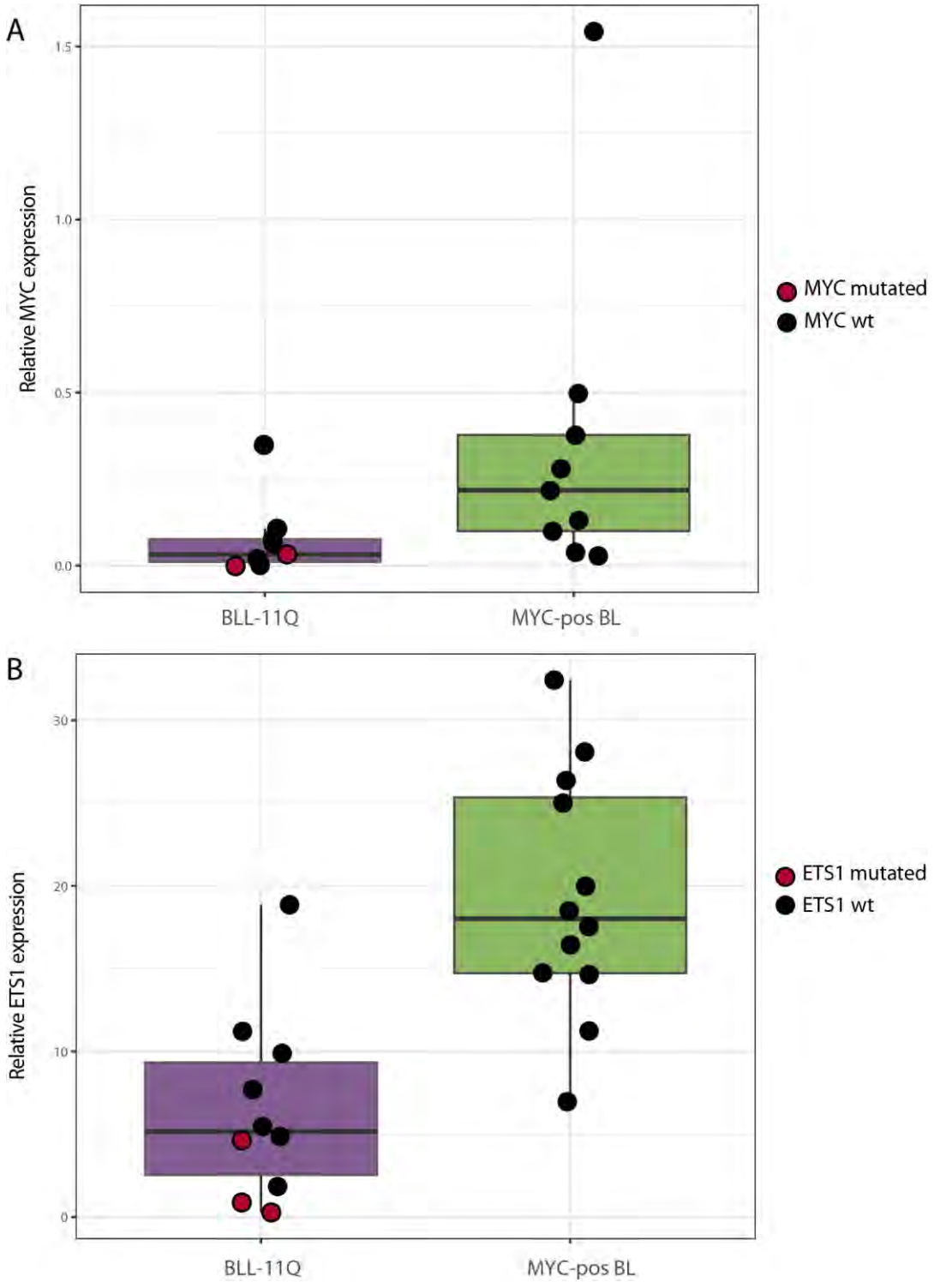

Supplementary Figure S5. Ideogram of chromosome 11q arm of 11 *MYC*-negative cases harboring 11q aberration by CN array. Gains are represented in blue, red corresponds to losses and CNN-LOH are represented in yellow. Two minimal regions of gain (MRGs) and one minimal region of loss (MRL) are pointed with blue and red boxes, respectively, and the minimal region of amplification (MRA) is indicated with the green box.

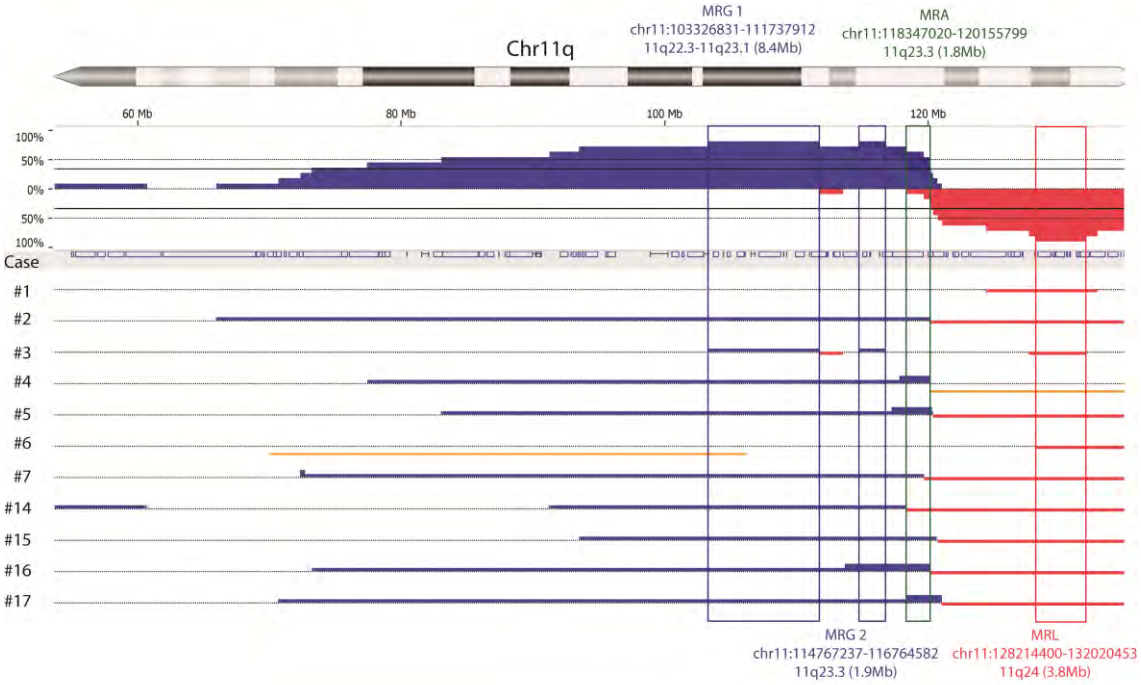

Supplementary Figure S6. Comparative plot of copy number aberrations between Burkitt-like lymphoma with 11q aberration (n=11) and **(A)** conventional *MYC*-positive Burkitt Lymphoma (n=35),[1] **(B)** GCB-Diffuse Large B-cell lymphoma (n=45)[5] and **(C)** ABC-Diffuse Large B-cell lymphoma (n=49)[5] X-axis depicts chromosome positions with dotted lines pointing centromeres. Y-axis indicates frequency of the genomic aberration among the analyzed cases. Significantly different regions of alterations among groups (Fisher test non-adjusted $P \leq 0.01$) are labeled with corresponding color asterisks.

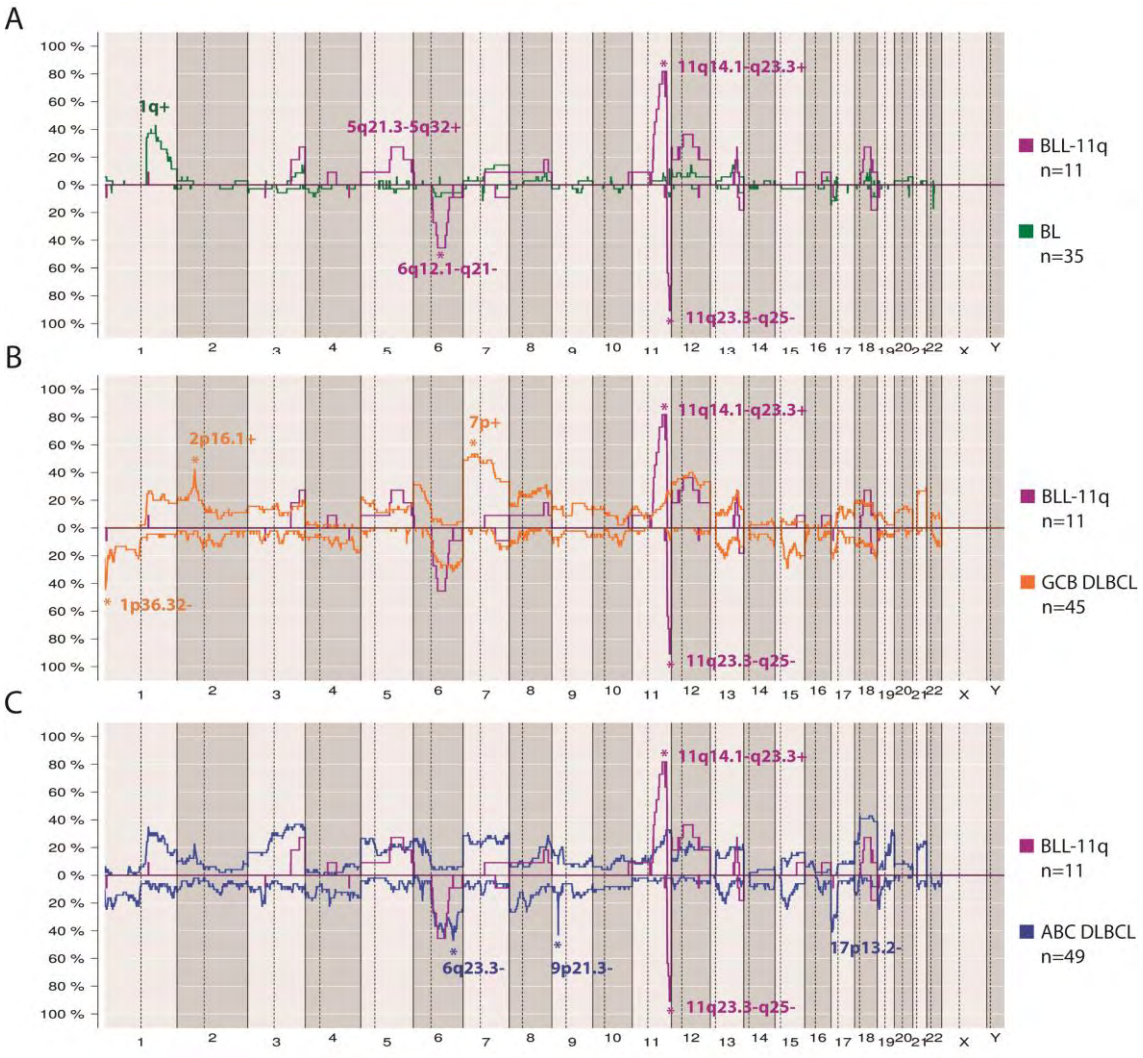

Supplementary Figure S7. (A) Comparative plot of copy number aberrations between Burkitt-like lymphoma with 11q aberration (n=11) and 6 *MYC*-negative 11q-negative cases **(B)** Mutational overview of 4 *MYC*-negative 11q negative cases in comparison with BLL with 11q aberration. The heat map shows the case specific pattern of driver mutations found by next generation sequencing. Each column represents a case and each row represents a gene. The right bar graph illustrates the mutation frequency of each gene.

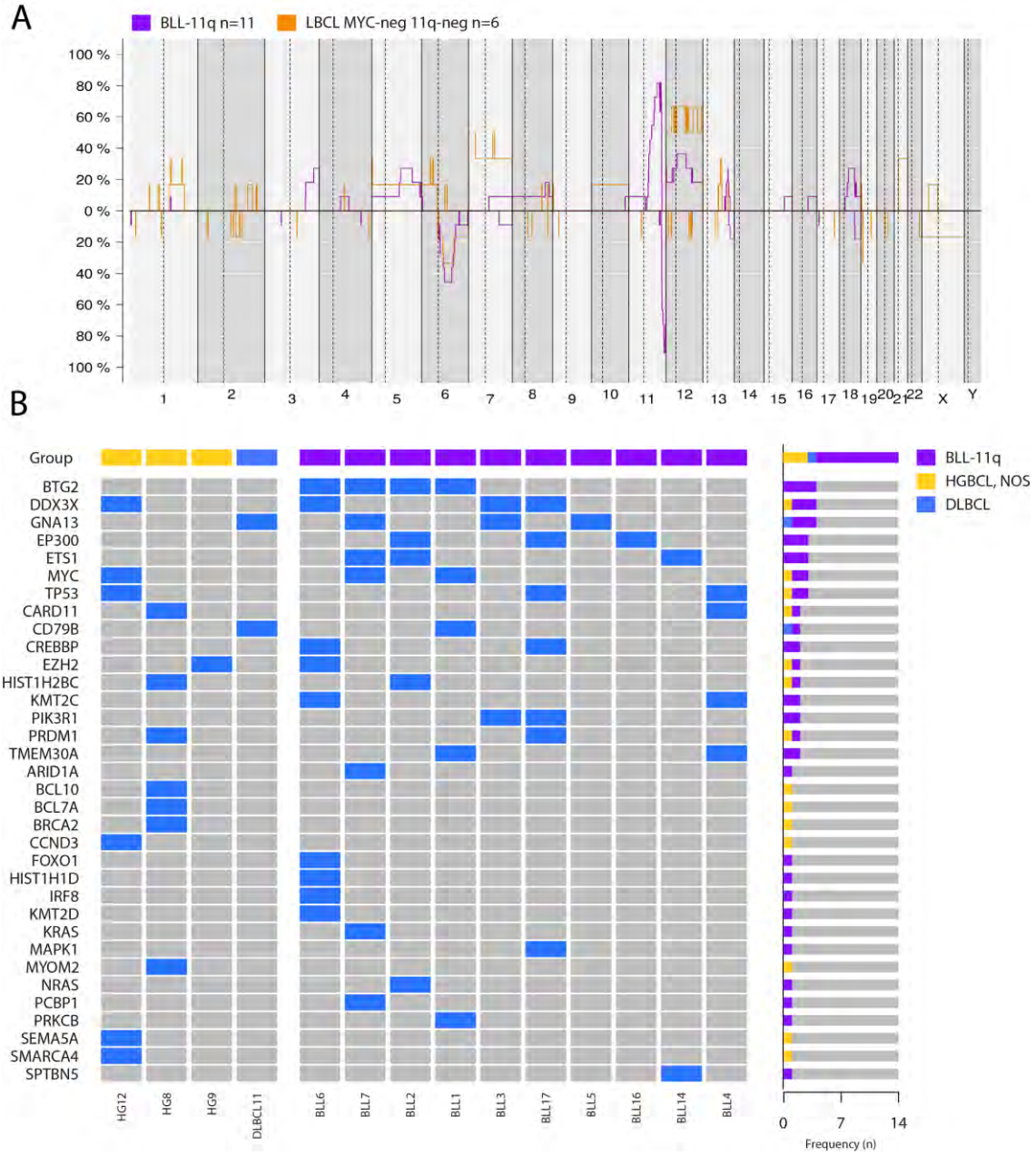

Supplementary Figure S8. Mean coverage distribution per gene of the 10 BLL-11q cases analyzed by target NGS. Y-axis indicates the mean number of reads. The red line depicts the mean coverage of all 10 cases. DNA from #2, #4 and #7 BLL-11q cases were extracted from frozen tissue.

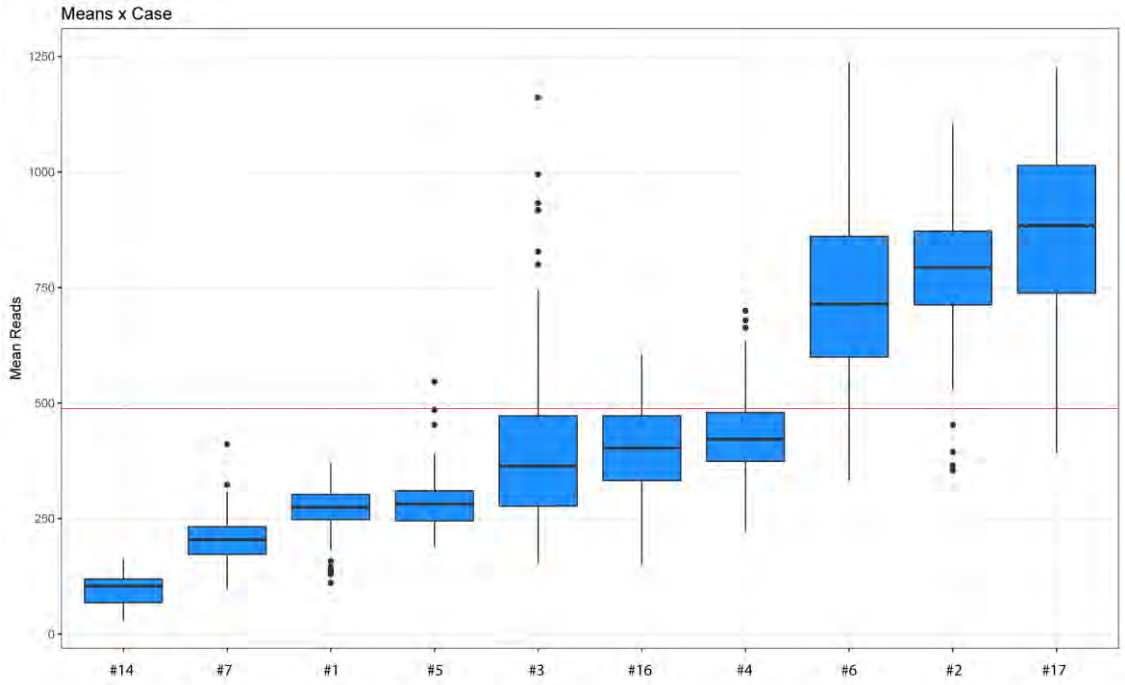

Supplementary Figure S9. NGS analysis pipeline followed to identify potential driver mutations in 10 BLL-11q samples. Two different variant callers were used: Somatic Variant Caller (Illumina) and Mutect2 (GATK version 4.0.3) and potential driver mutations were predicted according to previously published criteria.[5] SIFT predictor was only used for mutations in which a definitive score was not provided by Mutation Assessor.

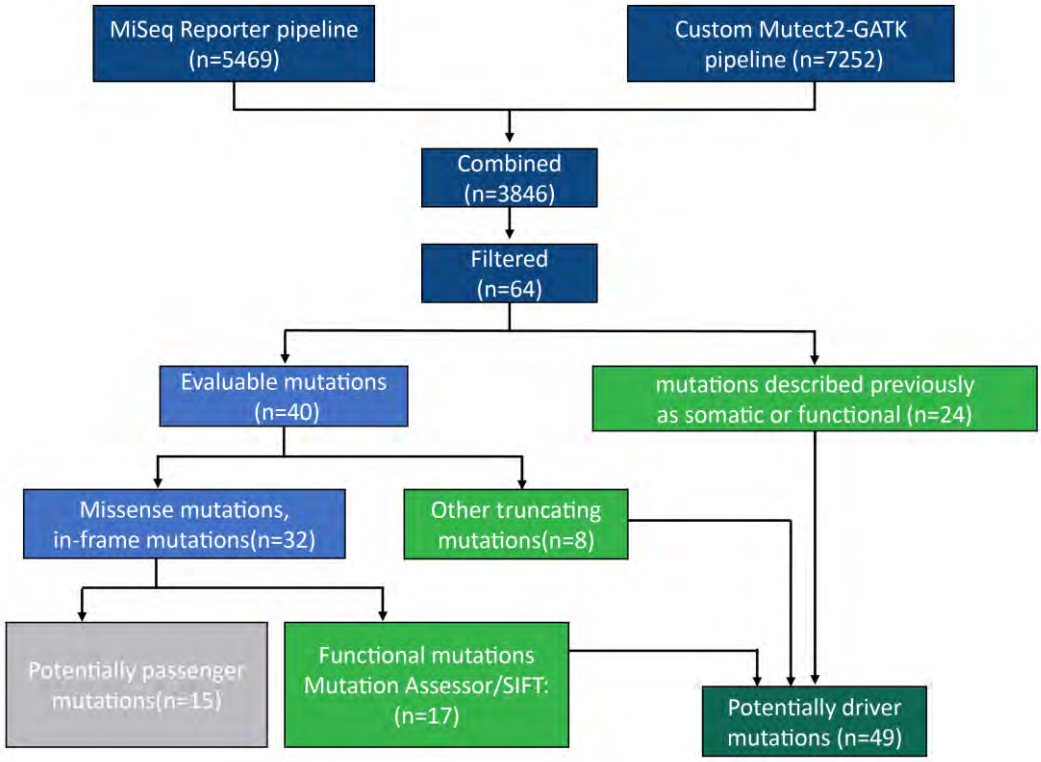

Supplementary Tables

Supplementary Table S1. Details of all antibodies used, source and conditions of use.

Antibody	Clone	Source	Antigen retrieval/visualization	Dilution
CD20	L26	DAKO, Copenhagen, Denmark	EDTA 1 mM pH 9/ ENVISION FLEX (DAKO)	RTU
CD79a	JCB 117	DAKO	EDTA 1 mM pH 9/ ENVISION FLEX (DAKO)	RTU
CD3	Polyclonal	DAKO	EDTA 1 mM pH 9/ ENVISION FLEX (DAKO)	RTU
CD5	4C7	DAKO	EDTA 1 mM pH 9/ ENVISION FLEX (DAKO)	RTU
CD10	56C6	DAKO	EDTA 1 mM pH 9/ ENVISION FLEX (DAKO)	RTU
BCL6	PG-B6p	DAKO	EDTA 1 mM pH 9/ ENVISION FLEX (DAKO)	RTU
BCL2	124	DAKO	EDTA 1 mM pH 9/ ENVISION FLEX (DAKO)	RTU
Ki67	Mib-1	DAKO	Citrate 10 mM pH 6/ ENVISION FLEX (DAKO	RTU
MUM1	MRQ-43	Ventana, Roche	CC1 solution / ultraView Universal DAB Detection Kit. Automated immunostainer (Benchmark XT; Ventana)	RTU
MYC*	Y69	Ventana, Roche	CC1 solution / ultraView Universal DAB Detection Kit. Automated immunostainer (Benchmark XT; Ventana)	RTU
LMO2*	1A9-1	Ventana, Roche, Tucson, AZ,USA	CC1 solution / ultraView Universal DAB Detection Kit. Automated immunostainer (Benchmark XT; Ventana)	RTU

RTU, ready to use.
*LMO2 was considered positive when >30% of the cells were positive and MYC was considered positive when more than 40% of positive tumor cells were observed, following the criteria of Colomo et al[17] and Johnson et al respectively.[18]

Supplementary Table S2. Ninety-six genes sequenced using Target NGS panel including references for inclusion in the mutational analysis and mean coverage by gene and amplicon.

Provided in excel format

Supplementary Table S3. Primers used for the verification of variants in *MYC, BTG2, ETS1* and *TP53* and the re-analysis *of ID3*, *TCF3* (exon 17) and *CCND3* (exon 5).

Primers *ETS1*					
Primer	**Sequence (5´-3´)**	**PCR product length (bp)**	**Case/Mutation**	**Variant**	**Mutation position (hg19)**
ETS1_1 F	CTGCAGGTCACACACAAAGC	157	BLL2	T>T/C	128332392
ETS1_1 R	TAAATTTCAGGTGGCCAGGA		BLL7	C>C/T	128332410
ETS1_5 F	CCACGGCTCAGTTTCTCATA	168	BLL2	A>A/T	128332477
ETS1_5 R	GGGTCACCATGAATGGGTAT				
ETS1_3 F	TTTGAATTCCCAGCCATCTC	167	BLL14	G>G/A	128333508
ETS1_3 F	GTGGGGATTAGCTGCGTAGA				
ETS1_E1F	GAAAGGGGGAAGAAGTCCAG	200	Exon 1 of transcript M_005238		
ETS1_E1R	CAAACTTGCTACCATCCCGTA				

Primers BTG2					
Primer	**Sequence (5´-3´)**	**PCR product length (bp)**	**Case/Mutation**	**Variant**	**Mutation position (hg19)**
BTG2_1F	GACATGAGCCACGGGAAG	228	BLL1	C>C/T	203274858
BTG2_1R	CTGCCGCAGGAGTAGAAGAA		BLL2	G>G/A	203274867
			BLL7	del	203274878

Primers *MYC*					
Primer	**Sequence (5´-3´)**	**PCR product length (bp)**	**Case/Mutation**	**Variant**	**Mutation position (hg19)**
MYC_2 F	GAGCTGCTGGGAGGAGACAT	150	BLL7	T>T/G	128750921
MYC_2 R	CTGGTAGGAGGCCAGCTTCT				
MYC_4 F	CTCCTGGCAAAAGGTCAGAG	158	BLL1	C>C/G	128752800
MYC_4 R	CCTCTTGGCAGCAGGATAGT				

Primers *TP53*					
Primer	**Sequence (5´-3´)**	**PCR product length (bp)**	**Case/Mutation**	**Variant**	**Mutation position (hg19)**
TP53_2 F	CCAGTGTGATGATGGTGAGG	163	BLL4	C>C/T	7577538
TP53_2 R	CCTGCTTGCCACAGGTCT				

Primers *ID3*			
Primer	**Sequence (5´-3´)**	**PCR product length (bp)**	**Reference**
ID3-FZ-F	TCCAGGCAGGCTCTATAAGTG	694	Rohde, et al[19]
ID3-FZ-R	CCGAGTGAGTGGCAATTTTT		Rohde, et al[19]
ID3-PE-F	GCTTACCTGGATGGGAAGGT	204	
ID3-PE-R	GAGGAGCCGCTGAGCTTG		

Primers *TCF3*			
Primer	**Sequence (5´-3´)**	**PCR product length (bp)**	**Reference**
TCF3-FZ-F	TGCTGTGCCCACCAATGTAAG CCATG	609	Rohde, et al[19]
TCF3-FZ-R	GTGGAGGCTTGTAAAGAAGAG AGTGG		Rohde, et al[19]
TCF3-PE-F	CAGGATGAGCAGCTTGGTCT	180	
TCF3-PE-R	AGTACGGACGAGGTGCTGTC		

Primers *CCND3*			
Primer	**Sequence (5´-3´)**	**PCR product length (bp)**	**Reference**
CCND3-FZ-F	CCATGTGTTGGGAGCTGTC	328	Rohde, et al[19]
CCND3-FZ-R	CTGGAGGCAGGGAGGTG		Rohde, et al[19]
CCND3-PE-F	GCCCCTCCTCTGCTTAGTG	198	
CCND3-PE-R	CTGTCAGGAGCAGATCGAAG		

Bp: base pairs; F: forward, R: reverse

Supplementary Table S4. Taqman assays used for qPCR analyses. (Applied Biosystems inc)

Gene Symbol	Assay ID	Amplicon size (bp)	Reference sequence
ETS1	Hs00428293_m1	99	NM_005238
MYC	Hs00153408_m1	107	NM_002467
B2M	Hs00984230_m1	81	NM_004048

Supplementary Table S5. Summary of copy number findings and FISH pattern constellation of the 11q aberration in the current series of BLL-11q.

Case	CN array		11q FISH (CEP11 [D11Z1] + RP11-414G21+RP11-629A20)	
	Pattern of chr11	**Number of alterations**	**11q FISH constellation pattern**[20]	**11q FISH result**
#1	Only terminal loss	2 CNA	nuc ish (D11Z1x2,RP11-414G21x2,RP11-629A20x1)	Only terminal loss
#2	Gain/terminal loss	3 CNA	nuc ish (D11Z1x2,RP11-414G21x2,RP11-629A20x1)	Only terminal loss
#3	Gain/terminal loss	6 CNA, 1 CNN-LOH	nuc ish (D11Z1x2,RP11-414G21x2-3,RP11-629A20x1)	Gain*/terminal loss
#4	Gain/amplification/CNN-LOH	15 CNA+ 1CNN-LOH	nuc ish (D11Z1x2,RP11-414G21x2-5,RP11-629A20x2)	Amplification
#5	Gain/amplification/terminal loss	4 CNA	nuc ish (D11Z1x2,RP11-414G21x4-5,RP11-629A20x1)	Amplification/terminal loss
#6	Only terminal loss	6 CNA + 11 CNN-LOH	nuc ish (D11Z1x2,RP11-414G21x2,RP11-629A20x1)	Only terminal loss
#7	Gain/terminal loss	8 CNA	nuc ish (D11Z1x2,RP11-414G21x3,RP11-629A20x1)	Gain/terminal loss
#14	Gain/terminal loss	4 CNA	nuc ish (D11Z1x2,RP11-414G21x2,RP11-629A20x1)	Only terminal loss
#15	Gain/terminal loss	12 CNA + 1CNN-LOH	Not done	
#16	Gain/amplification/ terminal loss	4 CNA	nuc ish (D11Z1x2,RP11-414G21x3,RP11-629A20x1)	Gain/terminal loss
#17	Gain/amplification/ terminal loss	14 CNA +3 CNN-LOH	nuc ish (D11Z1x2,RP11-414G21x3-4,RP11-629A20x1)	Amplification* /terminal loss

CNA: copy number alteration. CNN-LOH: copy number neutral loss of heterozygosity. *Only observed in a few cells. CN and FISH results were not concordant in cases #2, and #14 most likely due to the fact that gained region covered by BAC RP11-414G21 was most likely inverted and then both copies were very narrow to be clearly distinguished as independent signals in the FISH constellation.

Supplementary Table S6. Global table of copy number and copy number neutral of heterozygosity (CNN-LOH) alterations of the 11 BLL-11q aberration and the 6 MYC-negative 11q-negative cases.

Case	Array	Chromosome Region (Hg19)	Event	Length (bp)	Cytoband
#1					
	Oncoscan	chr6:67,759,432-110,118,776	CN Loss	42359345	q12 - q21
	Oncoscan	chr11:124,440,617-132,877,670	CN Loss	8437054	q24.2 - q25
#2					
	Cytoscan	chr6:302,273-3,157,193	CN Gain	2854921	p25.3 - p25.2
	Cytoscan	chr11:66,015,813-120,252,657	CN Gain	54236845	q13.2 - q23.3
	Cytoscan	chr11:120,253,875-135,006,516	CN Loss	14752642	q23.3 - q25
#3					
	Oncoscan	chr5:1-180,915,260	CN Gain	180915260	p15.33 - q35.3
	Oncoscan	chr11:103,326,831-111,737,912	CN Gain	8411082	q22.3 - q23.1
	Oncoscan	chr11:111,747,297-113,562,039	CN Loss	1814743	q23.1 - q23.2
	Oncoscan	chr11:114,767,237-116,764,582	CN Gain	1997346	q23.3
	Oncoscan	chr11:127,681,132-132,020,453	CN Loss	4339322	q24.2 - q25
	Oncoscan	chr17:40,114,049-81,195,210	CNN-LOH	41081162	q21.2 - q25.3
	Oncoscan	chr18:20,935,833-78,007,784	CN Gain	57071952	q11.2 - q23
#4					
	SNP6	chr3:148,377,370-198,022,430	CN Gain	49645061	q24 - q29
	SNP6	chr4:151,106,726-151,889,624	CN Loss	782899	q31.3
	SNP6	chr6:62,787,661-63,773,155	CN Loss	985495	q11.1 - q12
	SNP6	chr6:66,807,178-136,034,966	CN Loss	69227789	q12 - q23.3
	SNP6	chr6:137,582,049-168,332,407	CN Loss	30750359	q23.3 - q27
	SNP6	chr6:168,596,580-171,115,067	CN Loss	2518488	q27
	SNP6	chr8:118,905,307-134,171,629	CN Gain	15266323	q24.11 - q24.22
	SNP6	chr11:77,429,089-117,851,837	CN Gain	40422749	q14.1 - q23.3
	SNP6	chr11:117,851,837-120,155,799	High Copy Gain	2303963	q23.3
	SNP6	chr11:120,155,799-135,006,516	CNN-LOH	14850718	q23.3 - q25
	SNP6	chr12:40,494,911-93,085,645	CN Gain	52590735	q12 - q22
	SNP6	chr12:93,085,646-95,374,851	CN Loss	2289206	q22
	SNP6	chr12:95,374,851-96,373,225	CN Gain	998375	q22 - q23.1
	SNP6	chr18:29,031,540-56,749,287	CN Gain	27717748	q12.1 - q21.32
	SNP6	chr18:56,749,288-78,077,248	CN Loss	21327961	q21.32 - q23
	SNP6	chr19:6,700,469-6,935,092	CN Loss	234624	p13.3 - p13.2

Case	Array	Chromosome Region (Hg19)	Event	Length (bp)	Cytoband
#5					
	Oncoscan	chr6:78,975,348-114,942,024	CN Loss	35966677	q14.1 - q22.1
	Oncoscan	chr11:83,088,730-117,240,357	CN Gain	34151628	q14.1 - q23.3
	Oncoscan	chr11:117,242,677-120,392,430	High Copy Gain	3149754	q23.3
	Oncoscan	chr11:120,398,613-134,938,847	CN Loss	14540235	q23.3 - q25
#6					
	Oncoscan	chr1:150,029,936-151,599,267	High Copy Gain	1569332	q21.2 - q21.3
	Oncoscan	chr1:151,744,168-249,212,878	CNN-LOH	97468711	q21.3 - q44
	Oncoscan	chr3:117,248,700-124,701,188	CNN-LOH	7452489	q13.31 - q21.2
	Oncoscan	chr3:177,647,728-197,852,564	CN Gain	20204837	q26.32 - q29
	Oncoscan	chr4:124,989,820-147,017,448	CNN-LOH	22027629	q28.1 - q31.22
	Oncoscan	chr5:38,139-5,124,613	CNN-LOH	5086475	p15.33 - p15.32
	Oncoscan	chr5:76,061,256-96,465,623	CNN-LOH	20404368	q13.3 - q15
	Oncoscan	chr5:171,201,195-180,698,312	CNN-LOH	9497118	q35.1 - q35.3
	Oncoscan	chr8:79,796,337-94,671,697	CNN-LOH	14875361	q21.12 - q22.1
	Oncoscan	chr9:204,738-10,275,857	CNN-LOH	10071120	p24.3 - p23
	Oncoscan	chr11:70,045,922-106,288,554	CNN-LOH	36242633	q13.3 - q22.3
	Oncoscan	chr11:128,214,400-134,938,847	CN Loss	6724448	q24.3 - q25
	Oncoscan	chr12:189,400-133,818,115	CN Gain	133628716	p13.33 - q24.33
	Oncoscan	chr13:91,639,578-92,147,712	CN Gain	508135	q31.3
	Oncoscan	chr14:54,084,642-76,110,632	CNN-LOH	22025991	q22.1 - q24.3
	Oncoscan	chr18:59,650,717-62,178,511	CN Gain	2527795	q21.33 - q22.1
	Oncoscan	chr18:55,902,055-66,218,776	CNN-LOH	10316722	q21.31 - q22.1
#7					
	Cytoscan	chr1:5,195,097-7,019,203	CN Loss	1824107	p36.32 - p36.31
	Cytoscan	chr3:60,388,322-60,712,277	CN Loss	323956	p14.2
	Cytoscan	chr5:104,762,975-174,135,222	CN Gain	69372248	q21.3 - q35.2
	Cytoscan	chr5:178,688,093-180,719,789	CN Gain	2031697	q35.3
	Cytoscan	chr11:72,390,640-72,717,317	High Copy Gain	326678	q13.4
	Cytoscan	chr11:72,717,332-119,682,209	CN Gain	46964878	q13.4 - q23.3
	Cytoscan	chr11:119,682,255-134,938,470	CN Loss	15256216	q23.3 - q25
	Cytoscan	chr12:1-133,851,895	CN Gain	133851895	p13.33 - q24.33

Case	Array	Chromosome Region (Hg19)	Event	Length (bp)	Cytoband
#8					
	Oncoscan	chr1:23,506,625-23,985,309	CN Loss	478685	p36.12 - p36.11
	Oncoscan	chr1:116,776,586-118,300,350	CN Loss	1523765	p13.1 - p12
	Oncoscan	chr1:189,763,755-200,583,380	CN Gain	10819626	q31.1 - q32.1
	Oncoscan	chr2:180,790,820-198,749,269	CN Gain	17958450	q31.3 - q33.1
	Oncoscan	chr6:204,909-57,305,822	CN Gain	57100914	p25.3 - p11.2
	Oncoscan	chr6:57,329,886-58,055,927	CN Loss	726042	p11.2
	Oncoscan	chr6:58,213,475-58,770,502	CN Gain	557028	p11.2 - p11.1
	Oncoscan	chr6:61,886,393-170,913,051	CN Loss	109026659	q11.1 - q27
	Oncoscan	chr7:1-159,138,663	CN Gain	159138663	p22.3 - q36.3
	Oncoscan	chr7:1-159,138,663	CNN-LOH	159138663	p22.3 - q36.3
	Oncoscan	chr8:55,457,188-71,067,368	CN Loss	15610181	q11.23 - q13.3
	Oncoscan	chr9:204,738-35,809,328	CNN-LOH	35604591	p24.3 - p13.3
	Oncoscan	chr9:21,901,263-22,056,499	Homozygous Copy Loss	155237	p21.3
	Oncoscan	chr11:45,810,652-46,460,038	CN Loss	649387	p11.2
	Oncoscan	chr12:189,400-8,447,618	CN Loss	8258219	p13.33 - p13.31
	Oncoscan	chr12:19,557,354-21,282,570	CN Loss	1725217	p12.3 - p12.2
	Oncoscan	chr12:21,295,612-29,285,577	CN Gain	7989966	p12.2 - p11.22
	Oncoscan	chr12:30,814,259-33,886,138	CN Gain	3071880	p11.21 - p11.1
	Oncoscan	chr12:39,204,714-70,880,468	CN Gain	31675755	q12 - q15
	Oncoscan	chr12:74,309,125-77,911,802	CN Gain	3602678	q21.1 - q21.2
	Oncoscan	chr12:79,610,263-82,677,229	CN Gain	3066967	q21.2 - q21.31
	Oncoscan	chr12:84,462,140-89,275,759	CN Loss	4813620	q21.31 - q21.33
	Oncoscan	chr12:91,825,095-94,371,476	CN Loss	2546382	q21.33 - q22
	Oncoscan	chr12:98,498,625-115,061,325	CN Gain	16562701	q23.1 - q24.21
	Oncoscan	chr12:128,397,472-133,818,115	CN Gain	5420644	q24.32 - q24.33
	Oncoscan	chr13:45,901,876-53,198,648	CN Loss	7296773	q14.13 - q14.3
	Oncoscan	chr13:58,291,792-69,716,364	CN Gain	11424573	q21.1 - q21.33
	Oncoscan	chr20:29,519,156-40,272,376	CN Loss	10753221	q11.21 - q12
	Oncoscan	chrX:1-155,270,560	CN Loss	155270560	p22.33 - q28
#9					
	Oncoscan	chr5:1-180,915,260	CN Gain	180915260	p15.33 - q35.3
	Oncoscan	chr6:204,909-52,036,300	CNN-LOH	51831392	p25.3 - p12.2
	Oncoscan	chr6:32,100,302-32,998,152	High Copy Gain	897851	p21.32
	Oncoscan	chr7:41,421-159,118,443	CN Gain	159077023	p22.3 - q36.3
	Oncoscan	chr12:1-133,851,895	CN Gain	133851895	p13.33 - q24.33
	Oncoscan	chr17:40,424,255-80,263,427	CNN-LOH	39839173	q21.2 - q25.3
	Oncoscan	chr17:62,949,100-63,165,077	Homozygous Copy Loss	215978	q24.1
	Oncoscan	chr21:14,375,361-48,045,085	CN Gain	33669725	q11.2 - q22.3

Case	Array	Chromosome Region (Hg19)	Event	Length (bp)	Cytoband
#10					
	Oncoscan	chr17:400,959-12,159,990	CNN-LOH	11759032	p13.3 - p12
#11					
	SNP6	chr1:73,100,845-74,442,581	CN Gain	1341737	p31.1
	SNP6	chr1:149,962,792-152,551,299	CN Gain	2588508	q21.2 - q21.3
	SNP6	chr6:40,083,170-42,855,926	CN Gain	2772757	p21.2 - p21.1
	SNP6	chr6:78,166,644-117,921,913	CN Loss	39755270	q14.1 - q22.1
	SNP6	chr8:106,741,322-107,876,319	CN Gain	1134998	q23.1
	SNP6	chr8:128,951,273-129,358,847	CN Gain	407575	q24.21
	SNP6	chr9:223,542-3,003,015	CN Gain	2779474	p24.3 - p24.2
	SNP6	chr12:0-133,851,895	CN Gain	133851896	p13.33 - q24.33
	SNP6	chr13:56,118,024-57,280,068	CN Gain	1162045	q21.1
	SNP6	chr13:91,986,235-92,361,312	CN Gain	375078	q31.3
	SNP6	chr17:49,745,106-81,195,210	CNN-LOH	31450105	q21.33 - q25.3
	SNP6	chr19:1-12,492,039	CNN-LOH	12492039	p13.3 - p13.2
	SNP6	chr19:6,493,673-7,463,666	Homozygous Copy Loss	969994	p13.3 - p13.2
	SNP6	chr19:37,006,258-37,414,445	CN Loss	408188	q13.12
	SNP6	chr21:14,369,207-48,129,895	CN Gain	33760689	q11.2 - q22.3
#12					
	Oncoscan	chr1:144,790,037-193,932,788	CN Gain	49142752	q21.1 - q31.3
	Oncoscan	chr2:134,242,471-139,641,542	CN Gain	5399072	q21.2 - q22.1
	Oncoscan	chr2:212,437,072-215,227,024	CN Gain	2789953	q34
	Oncoscan	chr3:63,411-60,777,554	CNN-LOH	60714144	p26.3 - p14.2
	Oncoscan	chr3:116,120,738-117,045,461	CN Loss	924724	q13.31
	Oncoscan	chr4:181,713,895-190,915,650	CN Loss	9201756	q34.3 - q35.2
	Oncoscan	chr5:38,139-1,985,845	CN Gain	1947707	p15.33
	Oncoscan	chr6:85,053,988-92,677,362	CN Gain	7623375	q14.3 - q15
	Oncoscan	chr7:88,362,639-94,444,750	CN Gain	6082112	q21.13 - q21.3
	Oncoscan	chr8:128,651,315-128,766,080	CN Gain	114766	q24.21
	Oncoscan	chr8:128,767,004-128,840,276	CN Loss	73273	q24.21
	Oncoscan	chr13:64,574,475-69,315,335	CN Gain	4740861	q21.31 - q21.33
	Oncoscan	chr17:400,959-19,497,890	CNN-LOH	19096932	p13.3 - p11.2
	Oncoscan	chr19:247,232-3,093,163	CN Gain	2845932	p13.3
	Oncoscan	chr22:42,109,917-51,213,826	CN Loss	9103910	q13.2 - q13.33

Case	Array	Chromosome Region (Hg19)	Event	Length (bp)	Cytoband
#13					
	Oncoscan	chr7:41,421-24,971,213	CN Gain	24929793	p22.3 - p15.3
	Oncoscan	chrX:25,296,129-58,470,802	CN Gain	33174674	p21.3 - p11.1
	Oncoscan	chr10:567,325-135,434,303	CN Gain	134866979	p15.3 - q26.3
	Oncoscan	chr4:91,749,811-91,794,821	CN Gain	45011	q22.1
	Oncoscan	chr1:104,446,681-110,195,901	CN Gain	5749221	p21.1 - p13.3
	Oncoscan	chr1:110,200,360-110,240,929	CN Gain	40570	p13.3
	Oncoscan	chr12:189,400-133,818,115	CN Gain	133628716	p13.33 - q24.33
	Oncoscan	chr2:32,757,598-37,578,208	CN Loss	4820611	p22.3 - p22.2
	Oncoscan	chr2:121,588,532-129,317,105	CN Loss	7728574	q14.2 - q14.3
	Oncoscan	chr2:137,910,175-151,016,074	CN Loss	13105900	q22.1 - q23.3
	Oncoscan	chr2:153,153,555-160,994,348	CN Loss	7840794	q23.3 - q24.2
	Oncoscan	chr19:247,232-11,674,294	CNN-LOH	11427063	p13.3 - p13.2
	Oncoscan	chr19:6,528,235-7,104,673	Homozygous Copy Loss	576439	p13.3 - p13.2
#14					
	Oncoscan	chr7:74,132,398-159,118,443	CN Gain	84986046	q11.23 - q36.3
	Oncoscan	chr11:1-60,760,530	CN Gain	60760530	p15.5 - q12.2
	Oncoscan	chr11:91,274,842-118,350,945	CN Gain	27076104	q14.3 - q23.3
	Oncoscan	chr11:118,352,769-134,938,847	CN Loss	16586079	q23.3 - q25
#15					
	Oncoscan	chr5:99,257,992-146,632,594	CN Gain	47374603	q21.1 - q32
	Oncoscan	chr6:63,365,565-123,492,278	CN Loss	60126714	q11.2 - q22.31
	Oncoscan	chr10:122,564,306-135,434,303	CN Gain	12869998	q26.12 - q26.3
	Oncoscan	chr11:93,515,058-120,717,000	CN Gain	27201943	q21 - q23.3
	Oncoscan	chr11:120,732,508-135,006,516	CN Loss	14274009	q23.3 - q25
	Oncoscan	chr12:189,400-1,896,956	CN Gain	1707557	p13.33
	Oncoscan	chr12:22,812,766-28,466,571	High Copy Gain	5653806	p12.1 - p11.22
	Oncoscan	chr12:28,476,847-64,720,693	CN Gain	36243847	p11.22 - q14.2
	Oncoscan	chr12:64,720,694-73,671,118	High Copy Gain	8950425	q14.2 - q21.1
	Oncoscan	chr13:85,803,897-99,955,533	CN Gain	14151637	q31.1 - q32.3
	Oncoscan	chr13:99,967,798-115,103,150	CN Loss	15135353	q32.3 - q34
	Oncoscan	chr16:58,143,392-90,195,538	CN Gain	32052147	q21 - q24.3
	Oncoscan	chr17:59,315,145-80,263,427	CNN-LOH	20948283	q23.2 - q25.3
#16					
	Oncoscan	chr6:83,574,391-120,108,162	CN Loss	36533772	q14.1 - q22.31
	Oncoscan	chr11:73,228,685-113,724,673	CN Gain	40495989	q13.4 - q23.2
	Oncoscan	chr11:113,733,111-120,176,979	High Copy Gain	6443869	q23.2 - q23.3
	Oncoscan	chr11:120,187,433-134,938,847	CN Loss	14751415	q23.3 - q25

Case	Array	Chromosome Region (Hg19)	Event	Length (bp)	Cytoband
#17					
	Oncoscan	chr3:149,230,137-197,852,564	CN Gain	48622428	q25.1 - q29
	Oncoscan	chr4:77,277,624-107,631,213	CN Gain	30353590	q21.1 - q24
	Oncoscan	chr7:111,092,478-159,118,443	CN Loss	48025966	q31.1 - q36.3
	Oncoscan	chr8:172,417-33,010,693	CNN-LOH	32838277	p23.3 - p12
	Oncoscan	chr8:1-146,364,022	CN Gain	146364022	p23.3 - q24.3
	Oncoscan	chr8:58,406,216-146,292,734	CNN-LOH	87886519	q12.1 - q24.3
	Oncoscan	chr11:70,719,897-118,343,378	CN Gain	47623482	q13.4 - q23.3
	Oncoscan	chr11:118,347,020-121,053,084	High Copy Gain	2706065	q23.3
	Oncoscan	chr11:121,062,860-134,906,706	CN Loss	13843847	q23.3 - q25
	Oncoscan	chr13:79,420,211-83,071,814	High Copy Gain	3651604	q31.1
	Oncoscan	chr13:83,098,518-94,240,082	CN Gain	11141565	q31.1 - q31.3
	Oncoscan	chr13:94,251,808-115,103,150	CN Loss	20851343	q31.3 - q34
	Oncoscan	chr15:74,343,354-102,397,317	CN Gain	28053964	q24.1 - q26.3
	Oncoscan	chr17:7,536,527-7,619,668	CN Loss	83142	p13.1
	Oncoscan	chr18:33,243,441-55,865,613	CN Gain	22622173	q12.2 - q21.31
	Oncoscan	chr18:55,893,217-78,007,784	CN Loss	22114568	q21.31 - q23
	Oncoscan	chr20:32,385,089-62,912,463	CNN-LOH	30527375	q11.22 - q13.33

Supplementary Table S7. List of somatic mutations in BLL-11q including prediction of amino acid changes that affect protein function (MA, SIFT, Polyphen2, CADD).

Provided in excel format.

Supplementary Table S8. Mutational patterns across different germinal center derived lymphoma subgroups including BL,[21,22] DLBCL,[5,23] DH/TH,[24,25] and HGBCL, NOS with or without *MYC* rearrangement.[25] The BL pattern includes mutations in BL-associated genes and the GCB-DLBCL pattern includes mutations associated with GCB phenotype according to literature. BLL-11q mutational pattern includes genes mutated in more than 2 BLL-11q cases, not included in the other two signatures.

Mutational patterns	**Gene**	**BLL-11q current series n=10 (%)**	**GCB-DLBCL n=83 (%)**	**HGBCL DH/TH n=44 (%)**	**HGBCL with or without *MYC*-R n=9 (%)**	**BL n=32 (%)**
BLL-11q	***BTG2***	40	4.8*	-	-	0*
	ETS1	30	1.2*	-	-	0*
	EP300	30	6*	6.8	0	0*
Burkitt Lymphoma	***ID3***	0	0	25	88.9*	59.4*
	TCF3	0	0	4.5	0	31.3
	CCND3	0	3,6	29.2[b]	22.2	9.4
	MYC	20	2.4	43.2	44.4	71.9*
	DDX3X	30	0[a]*	-	-	31.3
GCB-DLBCL	***KMT2D***	20	32.5	60[c]	-	6.3
	CREBBP	20	25.3	50	44.4	6.3
	TNFRSF14	0	20.5	20[c]	-	0
	B2M	0	20.5	10[c]	-	0
	EZH2	10	21.7	27.3	0	0
	GNA13	30	21.7	15[c]	-	9.4
	FOXO1	10	13.3	30[c]	-	6.3
	ACTB	0	13.3	-	-	0
	SOCS1	0	15.7	30[c]	-	0

* Significant differences of mutated gene prevalence between BLL-11q series and the other germinal center entities ($P<0.05$).

[a] Only in Morin et al series n=23. [b] Only in Momose et al. n=24. [c] Only in Evrard et al. n=20.

Supplementary References

1. Scholtysik R, Kreuz M, Klapper W et al. Detection of genomic aberrations in molecularly defined Burkitt's lymphoma by array-based, high resolution, single nucleotide polymorphism analysis. Haematologica. 2010;95(12):2047-2055.

2. Li H, Durbin R. Fast and accurate short read alignment with Burrows-Wheeler transform. Bioinformatics. 2009;25(14):1754-1760.

3. McKenna A, Hanna M, Banks E et al. The Genome Analysis Toolkit: a MapReduce framework for analyzing next-generation DNA sequencing data. Genome Res. 2010;20(9):1297-1303.

4. Wang K, Li M, Hakonarson H. ANNOVAR: functional annotation of genetic variants from high-throughput sequencing data. Nucleic Acids Res. 2010;38(16):e164.

5. Karube K, Enjuanes A, Dlouhy I et al. Integrating genomic alterations in diffuse large B-cell lymphoma identifies new relevant pathways and potential therapeutic targets. Leukemia. 2018;32(3):675-684.

6. Reva B, Antipin Y, Sander C. Predicting the functional impact of protein mutations: application to cancer genomics. Nucleic Acids Res. 2011;39(17):e118.

7. Kumar P, Henikoff S, Ng PC. Predicting the effects of coding non-synonymous variants on protein function using the SIFT algorithm. Nat Protoc. 2009;4(7):1073-1081.

8. Adzhubei IA, Schmidt S, Peshkin L et al. A method and server for predicting damaging missense mutations. Nat Methods. 2010;7(4):248-249.

9. Kircher M, Witten DM, Jain P et al. A general framework for estimating the relative pathogenicity of human genetic variants. Nat Genet. 2014;46(3):310-315.

10. Salaverria I, Royo C, Carvajal-Cuenca A et al. CCND2 rearrangements are the most frequent genetic events in cyclin D1(-) mantle cell lymphoma. Blood. 2013;121(8):1394-1402.

11. Bouska A, McKeithan TW, Deffenbacher KE et al. Genome-wide copy-number analyses reveal genomic abnormalities involved in transformation of follicular lymphoma. Blood. 2014;123(11):1681-1690.

12. Spina V, Khiabanian H, Messina M et al. The genetics of nodal marginal zone lymphoma. Blood. 2016;128(10):1362-1373.

13. Puente XS, Bea S, Valdes-Mas R et al. Non-coding recurrent mutations in chronic lymphocytic leukaemia. Nature. 2015;526(7574):519-24.

14. Lopez-Corral L, Sarasquete ME, Bea S et al. SNP-based mapping arrays reveal high genomic complexity in monoclonal gammopathies, from MGUS to myeloma status. Leukemia. 2012;26(12):2521-2529.

15. Paiva B, Mateos MV, Sanchez-Abarca LI et al. Immune status of high-risk smoldering multiple myeloma patients and its therapeutic modulation under LenDex: a longitudinal analysis. Blood. 2016;127(9):1151-1162.

16. Swerdlow SH, Campo E, Harris NL, Jaffe ES, Pileri SA, Stein H, Thiele J (Eds) WHO Classification of Tumours of Haematopoietic and Lymphoid Tissues. (Revised 4th edition) IARC: Lyon 2017.

17. Colomo L, Vazquez I, Papaleo N et al. LMO2-negative Expression Predicts the Presence of MYC Translocations in Aggressive B-Cell Lymphomas. Am J Surg Pathol. 2017;41(7):877-886.

18. Johnson NA, Slack GW, Savage KJ et al. Concurrent expression of MYC and BCL2 in diffuse large B-cell lymphoma treated with rituximab plus cyclophosphamide, doxorubicin, vincristine, and prednisone. J Clin Oncol. 2012;30(28):3452-3459.

19. Rohde M, Bonn BR, Zimmermann M et al. Relevance of ID3-TCF3-CCND3 pathway mutations in pediatric aggressive B-cell lymphoma treated according to the non-Hodgkin Lymphoma Berlin-Frankfurt-Munster protocols. Haematologica. 2017;102(6):1091-1098.

20. ISCN 2013: an international system for human cytogenetic nomenclature (2013). In: Shaffer Lisa G., McGowan-Jordan J, Schmid M, eds.: Karger; 2013.

21. Schmitz R, Young RM, Ceribelli M et al. Burkitt lymphoma pathogenesis and therapeutic targets from structural and functional genomics. Nature. 2012;490(7418):116-120.

22. Richter J, Schlesner M, Hoffmann S et al. Recurrent mutation of the ID3 gene in Burkitt lymphoma identified by integrated genome, exome and transcriptome sequencing. Nat Genet. 2012;44(12):1316-1320.

23. Morin RD, Mungall K, Pleasance E et al. Mutational and structural analysis of diffuse large B-cell lymphoma using whole-genome sequencing. Blood. 2013;122(7):1256-1265.

24. Evrard SM, Pericart S, Grand D et al. Targeted next generation sequencing reveals high mutation frequency of CREBBP, BCL2 and KMT2D in high-grade B-cell lymphoma with MYC and BCL2 and /or BCL6 rearrangements. Haematologica. 2018

25. Momose S, Weissbach S, Pischimarov J et al. The diagnostic gray zone between Burkitt lymphoma and diffuse large B-cell lymphoma is also a gray zone of the mutational spectrum. Leukemia. 2015;29(8):1789-1791.